

UNCLASSIFIED

AD NUMBER: ADB048384

LIMITATION CHANGES

TO:

Approved for public release; distribution is unlimited.

FROM:

Distribution limited to U.S. Government agencies only; (test and evaluation), March 1980. Other requests for this document must be referred to the Materials Laboratory, Nonmetallic Materials Division, Coatings, and Thermal Protection Materials Branch. AFWAL/MLBE, Wright-Patterson AFB, Ohio 45433.

AUTHORITY

ST-A AFWAL LTR, 31 MAY 1985

AD B048384

AUTHORITY: AFWAL Itg 31 MAY 85



✓

LEVEL # (2) 48-

AFWAL-TR-80-4017, PART 1

ADBO48384

# CHARGING CONTROL SATELLITE MATERIALS

## PART 1

General Electric Space Division  
Philadelphia, Pennsylvania 19101

MARCH 1980

TECHNICAL REPORT AFWAL-TR-80-4017, PART 1

Interim Report for Period 1 August 1978 to 31 October 1979

DTIC ELECTE  
S JUL 2 1980 D  
A

DDC FILE COPY

Distribution limited to U.S. Government agencies only; (test and evaluation), March 1980.  
Other requests for this document must be referred to the Materials Laboratory, Nonmetallic  
Materials Division, Coatings, and Thermal Protection Materials Branch, AFWAL/MLBE,  
Wright-Patterson AFB, Ohio 45433.

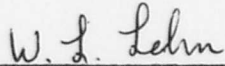
MATERIALS LABORATORY  
AIR FORCE WRIGHT AERONAUTICAL LABORATORIES  
AIR FORCE SYSTEMS COMMAND  
WRIGHT-PATTERSON AIR FORCE BASE, OHIO 45433

80 7 1 89

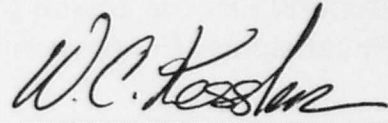
NOTICE

When Government drawings, specifications, or other data are used for any purpose other than in connection with a definitely related Government procurement operation, the United States Government thereby incurs no responsibility nor any obligation whatsoever, and the fact that the government may have formulated, furnished, or in any way supplied the said drawings, specifications, or other data, is not to be regarded by implication or otherwise as in any manner licensing the holder or any other person or corporation, or conveying any rights or permission to manufacture, use, or sell any patented invention that may in any way be related thereto.

This technical report has been reviewed and is approved for publication.




W.L. Lehn  
Project Engineer



W. Kessler, Chief  
Coatings and Thermal  
Protection Materials Branch

FOR THE COMMANDER:



F.D. Cherry, Acting Chief  
Nonmetallic Materials Division

"If your address has changed, if you wish to be removed from our mailing list, or if the addressee is no longer employed by your organization please notify AFWAL/MLBE, W-P AFB, OH 45433 to help us maintain a current mailing list".

Copies of this report should not be returned unless return is required by security considerations, contractual obligations, or notice on a specific document.

62102F

SECURITY CLASSIFICATION OF THIS PAGE (When Data Entered)

19 REPORT DOCUMENTATION PAGE		READ INSTRUCTIONS BEFORE COMPLETING FORM	
18	1. REPORT NUMBER AFWAL-TR-80-4017	2. GOVT ACCESSION NO. AD-8048384L	3. RECIPIENT'S CATALOG NUMBER
6	4. TITLE (and Subtitle) CHARGING CONTROL SATELLITE MATERIALS Part 1.	9	5. TYPE OF REPORT & PERIOD COVERED Interim rept. August 1978 - October 1979
10	7. AUTHOR(s) Ronald E. Schmidt	15	8. CONTRACT OR GRANT NUMBER(s) F33615-78-C-5119
	9. PERFORMING ORGANIZATION NAME AND ADDRESS General Electric, Space Division Philadelphia, Pennsylvania 19101		10. PROGRAM ELEMENT, PROJECT, TASK AREA & WORK UNIT NUMBERS Project 2422/82
	11. CONTROLLING OFFICE NAME AND ADDRESS Materials Laboratory (AFWAL/MLBE) Air Force Wright Aeronautical Laboratories (AFSC) Wright Patterson AFB, OH 45433	11	12. REPORT DATE March 1980
	14. MONITORING AGENCY NAME & ADDRESS (if different from Controlling Office) 12 82		13. NUMBER OF PAGES 73
			15. SECURITY CLASS. (of this report) Unclassified
			15a. DECLASSIFICATION/DOWNGRADING SCHEDULE
16. DISTRIBUTION STATEMENT (of this Report) Distribution limited to U. S. Government agencies only; (test and evaluation), March 1980. Other requests for this document must be referred to the Materials Laboratory, Nonmetallic Materials Division, Coatings and Thermal Protection Materials Branch, AFWAL/MLBE, Wright-Patterson AFB, Ohio 45433.			
17. DISTRIBUTION STATEMENT (of the abstract entered in Block 20, if different from Report)			
18. SUPPLEMENTARY NOTES			
19. KEY WORDS (Continue on reverse side if necessary and identify by block number) Electrical properties, spacecraft materials, static charge control, coating, space simulation, synchronous satellites, thin films, thermo-optical properties. Indium tin oxide, indium oxide, spacecraft charging.			
20. ABSTRACT (Continue on reverse side if necessary and identify by block number) Thin film coatings of indium oxide (IO) and indium tin oxide (ITO) on thin sheets of FEP Teflon and Kapton are evaluated as thin conductive transparent coatings. Deposition parameters necessary to optimize the coating surface resistance, solar absorptivity and stability are discussed in detail. Materials are coated over 30 cm square areas by reactive magnetron sputtering to achieve reproducible uniform			

405025

Handwritten initials/signature

coatings. Uniformity, deposition rate, coating thickness, oxygen partial pressure, insitu RF and DC biasing, and chamber conditioning are examined in detail. The charge control properties of the IO and ITO coated polymers are evaluated and demonstrated in a facility which provide a multiple energy electron radiation environment with energies up to 30 KeV at current densities in excess of  $2\text{nA}/\text{cm}^2$ .

sg cm

## FOREWORD

This report was prepared by the Space Division of the General Electric Company, Philadelphia, Pennsylvania, under Contract Number F33615-78-C-5119 for the Air Force Materials Laboratory. (The contract was initiated under Project Number 2422 Charging Control Satellite Materials). The work was administrated under the direction of the Coating and Thermal Protection Materials Branch, AFWAL/MLBE, Nonmetallic Materials Division, Materials Laboratory, Wright-Patterson Air Force Base, Ohio 45433. Dr. W. L. Lehn, served as the project engineer. This interim report covers work conducted during the first part of the program from 1 August 1978 to 31 October 1979. The manuscript was released for publication by the author in December 1979.

The program at General Electric was conducted by the Materials and Systems Survivability Engineering groups with Dr. Ronald E. Schmidt as the program manager. Mr. Ted Harris conducted the development of magnetron sputtering techniques for IO and ITO under the direction of Leo Amore and Dr. Schmidt. Mr. Harry Rauch was responsible for the conductive glass development.

Accession for	
NTIS Grant	<input checked="" type="checkbox"/>
DDC Tab	
Unprocessed Justification	
By _____	
Distribution/	
Availability Codes	
Dist	Avail and/or special
B	

# TABLE OF CONTENTS

Section		Page
I	INTRODUCTION . . . . .	1
	1. Background . . . . .	1
	2. Previous Programs . . . . .	2
	a. Change Control in Polymer Materials . . . . .	2
	b. Transparent Antistatic Satellite Materials . . . . .	3
	3. Program Description . . . . .	4
II	MATERIALS DEVELOPMENT . . . . .	5
	1. Approach . . . . .	5
	2. Indium Tin Oxide . . . . .	8
	a. Uniformity . . . . .	8
	b. Oxidation . . . . .	12
	c. Substrate . . . . .	16
	d. Reproducibility . . . . .	19
	e. Solar Cell Coverglasses . . . . .	23
	f. Other Substrates . . . . .	27
	3. Indium Oxide . . . . .	29
	a. DC Biasing . . . . .	30
	b. Comparison with ITO . . . . .	32
	4. Oxide Coating Stability . . . . .	36
	5. Coating Adhesion . . . . .	46
	6. Silica Nitride . . . . .	47
	7. Conductive Glass Development . . . . .	48
III	MATERIALS TESTING . . . . .	52
	1. Introduction . . . . .	52
	a. Large Area Test Facility . . . . .	53
	2. Vacuum Stability . . . . .	56
	3. Large Area Testing of ITO . . . . .	60
	4. Multiple Energy Exposure . . . . .	64
	5. Low Temperature Stability . . . . .	69
IV	CONCLUSIONS . . . . .	71

## LIST OF ILLUSTRATIONS

Figure		Page
1	Magnetron Sputtering Unit . . . . .	7
2	Transmittance and Reflectance of ITO Coated FEP Teflon . . . . .	9
3	Transmittance and Reflectance of ITO Coated 3 MIL Kapton . . . . .	9
4	Lichtenberg Figures in Aluminized Coating on Kapton . . . . .	11
5	Transmittance and Reflectance of ITO Coating on Microsheet . . . . .	11
6	Transmittance of ITO Coated Microsheet . . . . .	15
7	Absorptance of ITO Coated Microsheet. . . . .	15
8a	Percent Transmittance of 200Å ITO on Microsheet . . . . .	21
8b	Percent Reflectance of 200Å ITO on Microsheet . . . . .	21
9a	Percent Reflectance of 100Å ITO Coated Kapton (Aluminized) . . . . .	24
9b	Percent Reflectance of 100Å ITO Coated FEP Teflon (Silvered) . . . . .	24
10	Performance I-V Curve of 2 cm x 4 cm Solar Cell with ITO Coated Ce Doped (PPE) Coverglasses . . . . .	24
11	Performance I-V Curves of 2 x 4 Solar Cell Array with ITO Coated Ce Doped (PPE) Coverglasses . . . . .	25
12	Percent Transmittance of 100Å ITO Coated Coverglass . . . . .	28
13	Performance I-V Curve of 2 cm x 4 cm Solar Cell with 100Å ITO Coated Microsheet Coverglass . . . . .	28
14	Percent Transmittance of 100Å IO Coated 0211 Microsheet . . . . .	33
15	Percent Reflectance of 100Å IO Coated 0211 Microsheet . . . . .	33
16a	Humidity Test Setup (Top View) . . . . .	38
16b	Humidity Test Setup (Side View) . . . . .	38
17a	Combined Exposure Test Setup (Close-Up View) . . . . .	39
17b	Combined Exposure Test Setup (Total View) . . . . .	39
18a	Surface Resistance Stability of Reference Samples . . . . .	40
18b	Surface Resistance Stability of Kapton Reference Samples . . . . .	41
19	Solar Reflectance During Humidity Test . . . . .	43
20	Typical Surface Resistance Variation During Humidity Test (Kapton). . . . .	44
21	Environmental Stability to Combined Environment Exposure (ITO/Kapton) . . . . .	45
22	Environmental Stability to Combined Environment Exposure (I/O Kapton) . . . . .	45
23	Transmittance and Reflectance of Si <sub>3</sub> N <sub>4</sub> on Microsheet . . . . .	48
24a	Ribbon Forming Setup (Top View) . . . . .	50
24b	Ribbon Forming Setup (Side View) . . . . .	50
25	Thermal Expansion of GE-ITL . . . . .	51
26	Functional Diagram of ESD Test Facility . . . . .	52
27	Functional Diagram of Multi Beam Facility . . . . .	54
28	Schematic of Sample Configuration . . . . .	56

## LIST OF ILLUSTRATIONS (CONT'D)

Figure		Page
29	Actual Sample Configuration with Rotary Arm . . . . .	57
30a	ITO Coated FEP Teflon with Conductive Tape Ground Bond . . . . .	58
30b	Closeup of Conductive Tape Ground Bond on ITO Coated FEP Teflon . . . . .	58
31	1.3 Meter by 2.1 Meter Spacecraft Charging and Radiation Facility . . . . .	61
32	View of 12 Inch Square Sample Diagnostics Fixture . . . . .	61
33	Normalized Charging Characteristic of IO Coated Teflon and Kapton . . . . .	68
34	76 cm by 100 cm Cryopanel . . . . .	70

## LIST OF TABLES

Table		Page
1	Deposition Summary . . . . .	7
2	Surface Resistance of ITO Coated Microsheet . . . . .	14
3	Optical Properties of ITO Coated Microsheet . . . . .	16
4	Preliminary Surface Resistance Measurements of ITO Coated Substrates . . . . .	17
5	Average Surface Resistance of ITO Coated Substrates . . . . .	19
6	Optical Properties of ITO Coated Microsheet . . . . .	20
7	Surface Resistance of 100Å ITO Coatings . . . . .	22
8	Temporal Variation of 100Å ITO Coatings . . . . .	26
9	Properties of Initial 500Å Indium Oxide Coatings Using Magnetron Sputtering . . . . .	31
10	Properties of Indium Oxide Coatings Using Magnetron Sputtering with DC Biasing . . . . .	31
11	Properties of ITO Coatings Using Magnetron sputtering with DC Biasing . . . . .	34
12	Indium Tin Oxide (ITO) and Indium Oxide (IO) with DC Biasing . . . . .	34
13	Comparison of Conductive Coating Surface Resistance . . . . .	35
14	Preliminary Combined Exposure Results . . . . .	42
15	Summary of Current Resistance Measurements on 11.5 cm Diameter . . . . .	60
16	Summary of Current Measurements on One Foot Square Samples of ITO Coated FEP Teflon and Kapton . . . . .	63
17	Summary of Current Measurements on ITO Coated Kapton and Teflon Films . . . . .	63
18	Summary of Current Measurements on One Foot Square Samples of 100Å ITO Coated FEP Teflon and Kapton . . . . .	65
19	Summary of Current Measurements on 100Å Indium Oxide Coated Kapton and Teflon Films . . . . .	66
20	Summary of Currents from 100Å IO Coated Kapton and Teflon Films . . . . .	67

## SUMMARY

The object of the program described in this report was the continued development and optimization of conductive films on thermal control materials and conductive glass and grounding techniques on which we have already conducted exploratory development and demonstrated feasibility. One of the objectives is to establish process parameters on the coating process which would provide data to a scale up process to produce quantities of charge control materials for actual spacecraft hardware.

The work reported in Section II details the evaluation of the coatings in the major areas of concern for understanding and predicting the coating characteristics. The major areas of process and coating evaluation were identified as: 1) uniformity, 2) deposition rate, 3) coating thickness, 4) sputtering environment or oxygen partial pressure, 5) in situ RF or DC biasing, 6) chamber conditioning or history, and 7) differences between IO and ITO.

Reactive magnetron sputtering of indium oxide and indium tin oxides in thickness between  $100\text{\AA}$  and  $1000\text{\AA}$  have been successfully demonstrated. Extensive tests of the coating reproducibility and stability to combined temperature and humidity environments have lead to selection of an optimum coating thickness with low surface resistance and a solar absorptance of only one to two percent.

Thin tiles of conductive lithium lanthanum borosilicate glass tiles have been produced as ribbon glass and cut into 2.5 cm square tiles. Additional work is underway to improve on the flatness of the glass so that it can be polished for OSR application.

A new facility for simulating the electron plasma environment at geosynchronous altitudes is described in Section III. This facility is used to measure the performance of the IO and ITO coated polymers up to  $30\text{ cm}^2$  square under electron radiation by multiple energy electrons up to 30 KeV and current densities larger than  $2\text{ nA/cm}^2$ . The materials surface and bulk currents and voltages are measured as a function of the incident electron energies.

SECTION I  
INTRODUCTION

1. BACKGROUND

Synchronous altitude satellites have been observed to exhibit anomalous behavior not noted in low orbit spacecraft. These anomalies have included logic upsets, gradual temperature increases due to degradation of thermal control surfaces, electromagnetic interference (EMI) to communication links between the spacecraft and ground and in at least one case, catastrophic power system failure. Studies conducted on several DOD and commercial satellites found a high correlation between the anomalous events and high magnetic indices during the hours between midnight and 6 a. m. spacecraft local time.<sup>1</sup> These correlations indicate the problem is related to some geophysical phenomena that results in electrical discharges in the vicinity of or on spacecraft structural surfaces. It is now generally accepted that this phenomena is the occurrence of a magnetic substorm when the spacecraft is in the plasma sheath, a vast region of space extending from the side of the Earth opposite the Sun. This can result in a non-uniform distribution of charge on the external surface of the spacecraft.

The external surface of a spacecraft is complex and an extremely important subsystem of the satellite necessary for its adaption to the space environment. The most important factor is the thermal balance of the spacecraft within the environment. External surfaces control thermal balance through the ratio of their solar absorptance ( $\alpha_s$ ) to their emissivity ( $\epsilon$ ) (as referenced to a black body). In general, metals; i. e., conductors, have a high  $\alpha_s/\epsilon$  ratio and will tend to run hot when receiving solar radiation. As a result, dielectrics, which have lower  $\alpha_s/\epsilon$  are selected as thermal control surfaces to keep the spacecraft within a safe operating temperature.

When placed in an energetic electron plasma environment these external high dielectric materials will accumulate and support a high net charge and since dielectrics have extremely

---

<sup>1</sup>Spacecraft Charging at High Altitudes: SCATHA Satellite Program, D. A. McPherson, D. P. Cauffman and W. R. Schober, J. Spacecraft 12 621-626 (1975).

low charge mobility, the charge distribution will most likely be non-uniform. This non-uniform charge build-up leads to large potential differences and high electric fields between dielectrics sufficient to breakdown the material or generate vacuum arcs at the edges of the materials.

Laboratory tests have shown that electrical discharges such as those on metallized Kapton cause physical damage to dielectric materials used for satellite thermal control systems. Metallized and polymeric films, because of their use in large area applications and multi-layer configurations, are particularly vulnerable to static charge build-up and subsequent degradation from arcing. This arcing can cause removal of the metallized layer and vaporization of the polymeric film, thus severely degrading the optical properties of the material. Additionally this can cause contamination and degradation of adjacent thermal control, optical and other systems. Charge control techniques when applied to these surfaces must not significantly degrade the solar absorptance ( $\alpha_s$ ) or emissivity ( $\epsilon$ ) of the thermal control surface both upon initial application and after long term space exposure.

Several exploratory development programs sponsored by AFML have preceded this program to reduce or prevent the buildup of static charge on external spacecraft thermal control and power materials. These programs have developed and begun evaluating solutions in the major areas of charge control including:

1. Conductive coatings
2. Conductively modified bulk materials
3. Grounding techniques

## 2. PREVIOUS PROGRAMS

### a. CHARGE CONTROL IN POLYMER MATERIALS

As a result of the work performed on Exploratory Development of Static Charge Control Materials under Contract F33615-76-C-5075 several concepts were evaluated which would enable the control of static charge on spacecraft polymeric film materials. The program

considered FEP Teflon, with a second surface coating of aluminum or silver which is used as a heat rejecting, solar reflecting passive temperature coating, and aluminized Kapton which finds use as the outer covering of multilayer insulation blankets. These two dielectric materials can comprise over 90% of the outer covering of a spacecraft, excluding solar array panels.

Several techniques including conductive grids and thin film coatings of semiconductor metal oxides were investigated. The thin film coatings of indium oxide (IO) and indium-tin oxide (ITO) were found to give the most consistent results for low surface resistance sufficient to control static charge build up while providing a low solar absorptance. Several techniques were also investigated for depositing these materials onto varied geometries. These included: 1) vacuum vapor deposition, 2) chemical vapor deposition, 3) DC sputtering, 4) RF sputtering, and 5) magnetron S-gun sputtering. The final process was found to give the most consistent results with the lowest thermal affect on the sample.

A number of grounding configurations were introduced and tested including conductive metal tapes, conductive adhesives, adhesives with conductive fillers, and metal washers on ITO coated polymer films of FEP Teflon and Kapton.

#### b. TRANSPARENT ANTISTATIC SATELLITE MATERIALS

As a result of the work performed on Exploratory Development of Transparent Antistatic Satellite Materials under Contract F33615-76-C-5258 charge control materials and techniques applied to solar cell coverglasses and OSR mirrors were developed and tested. Several techniques were considered for use in transparent applications including use of the semiconductor metal oxides and modified glass compositions to achieve a high conductivity.

Transparent conductive coatings of indium oxide and indium/tin oxides were found to be the most promising candidates for their stability on fused silica and borosilicate glasses used in OSR and coverglass configurations. The use of chamfering was also demonstrated for improved grounding of the conductive surfaces.

### 3. PROGRAM DESCRIPTION

The above programs evaluated a large number of charge control techniques and did not emphasize extensive testing of any of the materials considered. Additional work therefore is required on these coatings to provide more data on their stability to the thermal, vacuum, and solar environment necessary to qualify their use as thermal control materials for use on long term spacecraft missions. Furthermore the scale up of these thin film charge control coatings need to be demonstrated from the small samples evaluated on the previous programs to sizes useful for spacecraft manufacturers. Therefore, a full parametric characterization of the deposition techniques including uniformity and substrate dependence is required for any scale up operation leading to a manufacturing application for flight hardware.

The objective of the work described in the following sections was to evaluate the process parameters and variability necessary to produce transparent conductive oxide coatings on typical satellite thermal control substrates. Emphasis was placed on the most promising candidates developed as of the conclusion of the previous contractual efforts. These candidates were identified as reactive deposition of indium oxide and indium tin oxide by magnetron sputtering. The following efforts have identified the reproducibility, uniformity, adhesion and stability of the coating. The evaluation has been based upon the performance of the optical properties and electrical properties of the coated substrates under storage, humidity, handling and simulated geosynchronous vacuum and electron plasma environments.

## SECTION II

### MATERIALS DEVELOPMENT

#### 1. APPROACH

The work described in this report represents the evaluation of conductive transparent coatings and the process development toward the optimization and characterization of thin semiconductor type oxide coatings on typical thermal control satellite materials. The objective has been directed towards determining the necessary process parameters and their variability for use in a scale up operation from the 15 cm diameter samples coated under earlier contractual efforts.<sup>2,3</sup> The work relies heavily on the previous accomplishments and has concentrated on the most promising candidates identified for conductive transparent coatings. These candidate materials are indium oxide and indium (~ 90%) tin (~ 10%) oxide in thin films of the order of 100 Å to 1000 Å thick.

The initial efforts concentrated on developing the process parameters and determining the allowable variation to achieve highly transparent and highly conductive coatings on large sample sizes up to 30 cm square. These process development characterizations considered deposition rate, reactive oxygen partial pressure and in situ biasing, coating thickness and sample size. This development has been evaluated in terms of the coating's solar absorptivity, surface resistance, stability of its shelf life, stability to tape and rubtests and charge control performance under simulated substorm environments.

Thin conductive films of indium tin oxide and indium oxide were evaluated on three types of substrates typical of external satellite dielectric materials. The materials considered were silvered and uncoated 125 μm (5 mil) FEP Teflon, aluminized and uncoated 75 μm (3 mil) Kapton and silvered and uncoated glass tiles. These materials represent flexible second surface mirror materials, external multilayer blanket insulation material, optical solar reflectors (OSR) and solar cell coverglasses.

---

<sup>2</sup> Spacecraft Static Charge Control Materials, A. Eagles, et al, AFML-TR-77-105 Part II, July 1978

<sup>3</sup> Transparent Antistatic Satellite Materials, A. Eagles, et al AFML-TR-77-174 Part II, July 1978

The depositions of the semiconductor oxides onto the substrate materials were made by reactive magnetron sputtering in a Varian 3120H sputtering system using a planetary fixture shown in Figure 1. The reactive deposit is accomplished by sputtering from the indium or indium-tin metal target in an oxygen atmosphere. Magnetron sputtering has been found to be a cooler process as compared to conventional vapor deposition techniques, this is an important factor for depositions onto thermally sensitive materials such as Teflon. The planetary fixture consists of three dishes inclined toward the target and in the shape of spherical segments about four inches deep which simultaneously rotate about their axes and about the sputtering target during the deposition. For coating the polymer materials a flat aluminum plate about 17 inches in diameter was mounted to the rim of the planetary dish to provide a suitable sample holder for large planar materials. Alternate approaches to a flat plate were evaluated to obtain a sample configuration which would provide a more uniform coating. This uniformity is controlled by the position of the sample with respect to the sputtering target.

In situ biasing of the planetary fixture with an RF energy during the deposition has been found to provide stable conductive transparent oxide coatings which do not require any post deposition annealing. Use of this RF activation is evaluated further. In addition DC biasing of the planetary is evaluated to achieve the same results since DC biasing in some cases is simpler and safer to operate. Occasional arcing from the in situ RF and DC activated planetary to the back surface metalization has been observed in some deposition runs and must be considered in any deposition using the enhanced field activation of the reactive sputtering process. The results of these arcing sometimes appear as Lichtenberg figures in the aluminized and silvered back surface coating around the edges of the Kapton and FEP Teflon samples and may be reduced by control of the bias power level.

Eleven depositions have been performed during this effort to obtain a process and coating characterization necessary to reproduce consistent conductive transparent oxide coatings. Table 1 summarizes the process of characterization for the development of stable highly transparent conductive coatings.



Figure 1. Magnetron Sputtering Unit

Table 1. Deposition Summary

Date	Deposition	Purpose	Comments
8/78	1	Initial deposit of ITO on 12" x 12" Polymer films Evaluate Uniformity across flat samples	300 $\text{\AA}$ 300 $\text{\AA}$ Samples sent to AFML
9/78	2	Evaluate effect of Oxygen and Carrier Gas (Ar) pressure on $\alpha$ & Rs of coating; Initial evaluation of coating thickness	
10/78	3	Further evaluation of $\alpha$ & Rs of thin coatings Variance in Rs for a particular deposition	100 $\text{\AA}$ -500 $\text{\AA}$ ITO 200 $\text{\AA}$ Samples sent to AFML
12/78	4	Reproducibility of coating ( $\alpha$ & Rs) between consecutive deposits	100 $\text{\AA}$ ITO Rs increased with back surface coating
1/79	5	Initial deposition of IO using magnetron sputtering	Deposits on glass; 500 $\text{\AA}$
2/79	6	Comparison of IO & ITO on small samples	Deposits made using DC Bias on all 3 substrates 100 $\text{\AA}$ , 300 $\text{\AA}$
3/79	7	Further evaluation of IO & ITO on small samples	
4/79	8	Initial Deposits of IO on 12" x 12" polymer films	100 $\text{\AA}$ Samples tested under electron irradiation
5/79	9	Evaluation of flash interface coatings to improve ITO & IO adhesion	
6/79	10	Extended Humidity and Temperature environment testing	
8/79	11	IO deposition on 0211 glass tiles for 12" x 12" OSR Matrix	

## 2. INDIUM-TIN OXIDE

### a. UNIFORMITY

The initial work on developing and optimizing conductive transparent coatings on glass and polymer substrates was directed toward establishing the large area characteristics of thin films of indium-tin oxide on samples up to 30 cm (12") by 30 cm (12").

The initial depositions in the S-Gun magnetron sputtering chamber were performed to measure the reproducibility of the deposition parameters to provide consistent transparent conductive coatings. The FEP Teflon and Kapton films were initially metalized with about 1500Å of their respective back surface reflector material.

The initial reactive deposition was of 300Å indium tin oxide (ITO) onto 30 cm (one foot) square sheets of FEP Teflon. The depositions were at a 1 Å/sec deposition rate with in situ RF radiation applied to the sample to improve the oxidation. Because of the relatively low melting temperature of the indium-tin target only about one percent of the available magnetron power was used during the deposition. Operation at higher power levels raise the temperature of the target and increase the probability of melting the metal target and electrically shorting the magnetron.

The resulting 300Å coatings were highly conductive in the center over approximately a 9" square area but were highly resistive around the perimeter of the sample. Repetition of the deposition using the same parameters as used initially but increasing the deposition rate to 2 Å/sec provided 300Å coatings which were highly transparent and conductive across the entire square foot area. Similarly, successful transparent and conductive coatings were also produced repeatedly on aluminized Kapton.

Figures 2 and 3 show the reflectance and transmittance of the unmetalized ITO coated 125 μm (5 mil) FEP Teflon and 75 μm Kapton. The figures show T and R for the uncoated and ITO coated polymers. Notice that the difference in scales between R and T do not show the 30% separation between R and T scales.

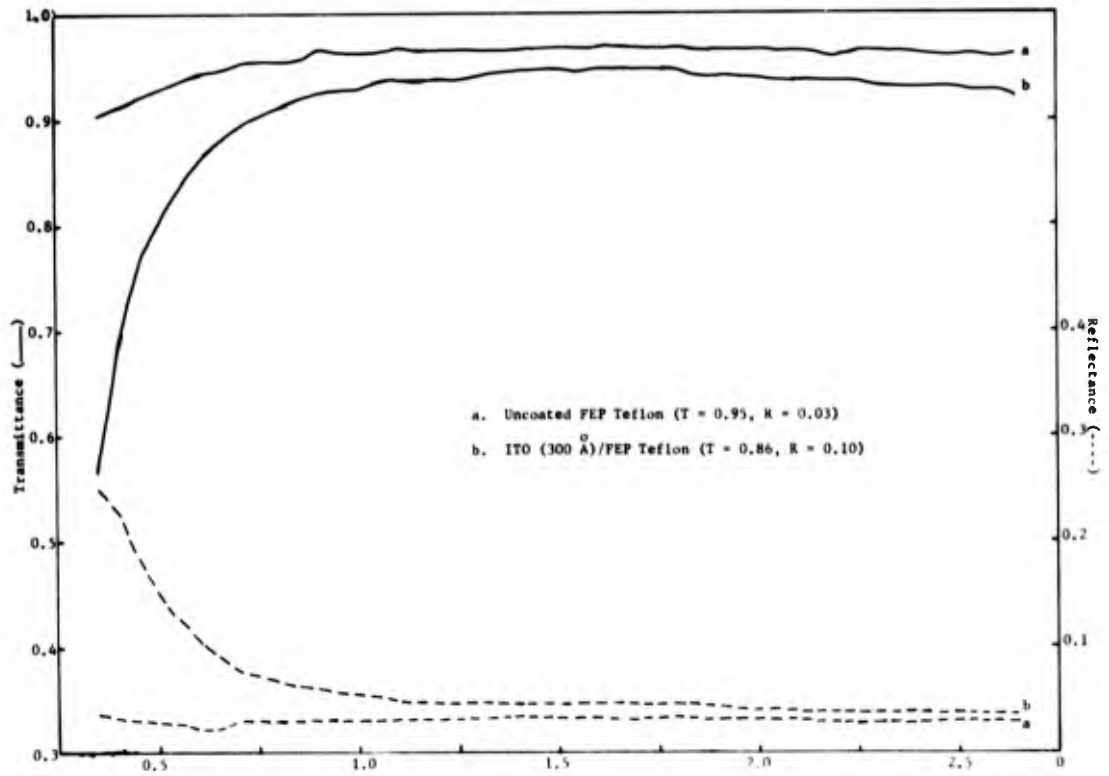


Figure 2. Transmittance and Reflectance of ITO Coated FEP Teflon

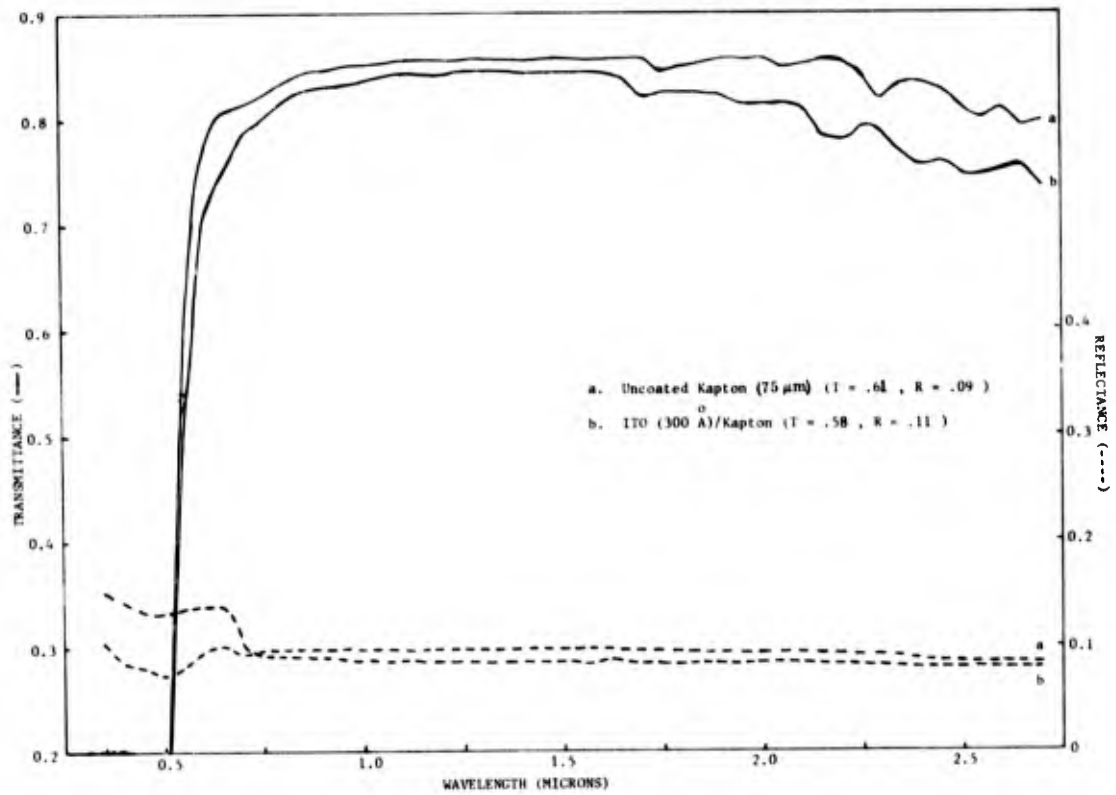


Figure 3. Transmittance and Reflectance of ITO Coated 3 Mil Kapton

Surface resistance measurements using a four point probe with a 0.2 inch spacing and assuming a constant geometry factor did show an increase in surface resistance from center to edge of the 12 inch sample even at the higher deposition rate. Typical surface resistance values on the ITO coated Kapton indicated a sheet resistance of about  $400 \Omega/\square$  in the center, increasing to about  $700 \Omega/\square$  on the sides and about  $2000 \Omega/\square$  on the corners. This decrease in surface resistance toward the center was also accompanied by a slight darkening of the film toward the center indicative of a lower oxide or greater metallic coating near the center. This non uniformity is probably due to the planar geometry of the film holder described above which places the center of the sample closer to the target than the edges. In this configuration the center experiences a slightly faster deposition rate and, therefore, a lower oxide reaction than the edges. An improved method of attachment which leads to more uniform coatings was developed during work on the indium oxide coatings and will be discussed in a later section.

As was mentioned in the previous section some arcing was observed in the RF biased planetary when the aluminized Kapton sample were being coated. Lichtenberg figures were evident in some of the back surface coatings. Figure 1 shows an example of this coating. Measurement of surface resistance of the ITO coatings over these figures show that the arcing had no effect on the ITO deposition. The arcing problem disappeared when the bias power level was reduced.

In addition to the deposition on the polymeric films  $300\text{\AA}$  thick coatings of ITO were reactively deposited on one inch squares of Corning 0211 microsheet. For these substrates the ITO coatings were applied before application of any back surface reflective coating. The glass tiles were mounted directly to the rotating planetary fixture since the large flat surface used for the polymer coatings was not required. Surface resistance measurements of the ITO coating on these tiles showed fairly uniform and consistent conductivity for all the tiles. In general the resistances using a four point probe and a HP 3450A multifunction meter were in the  $500$  to  $600 \Omega/\square$  range. Transmittance and reflectance measurements on a typical  $300\text{\AA}$  coated microsheet tile is shown in Figure 5. As observed in Figure 3 the effect of

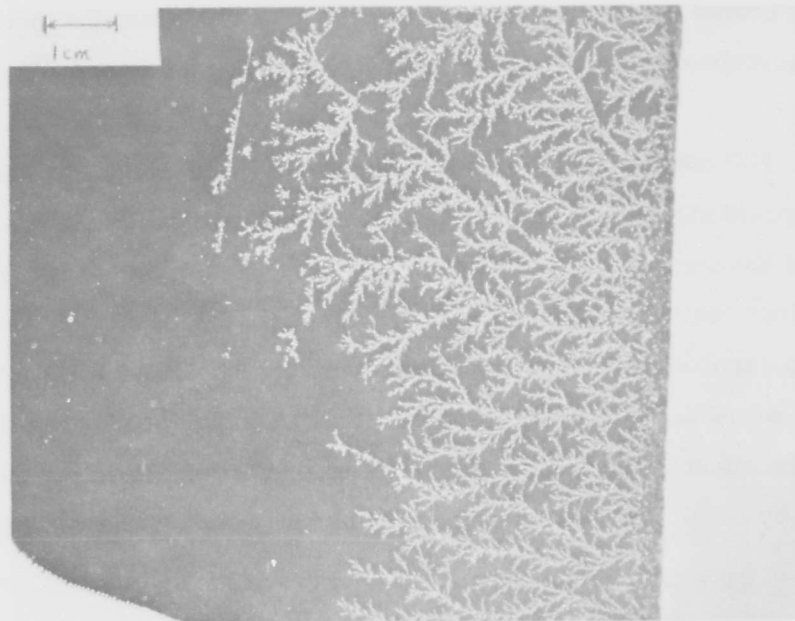


Figure 4. Lichtenberg Figure in Aluminized Coating on Kapton

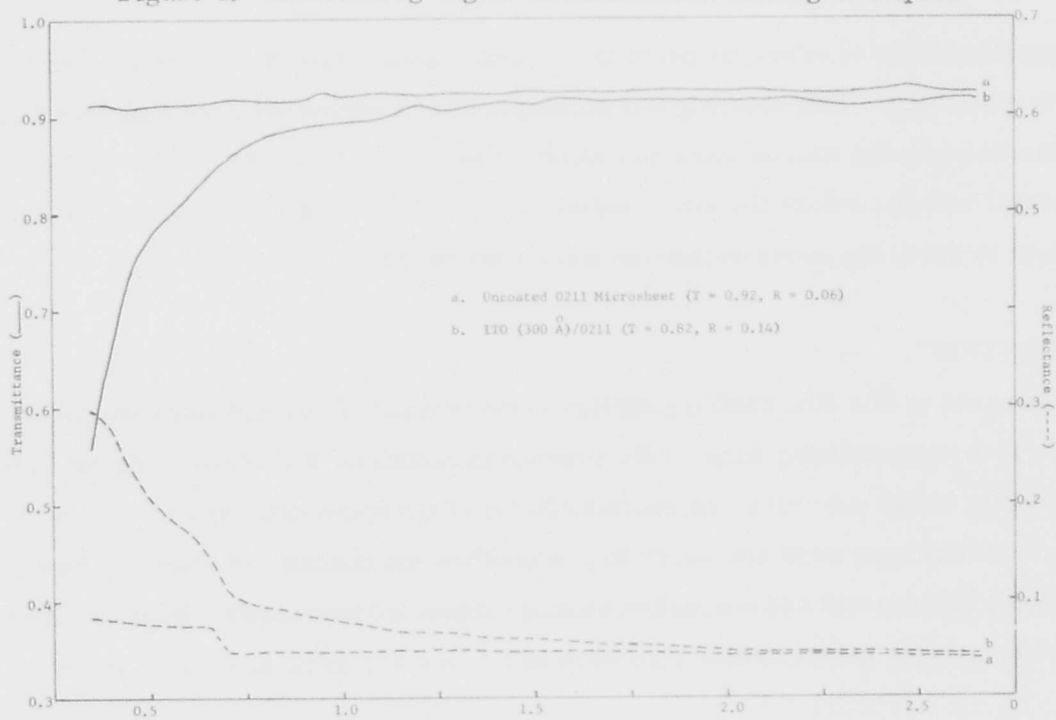


Figure 5. Transmittance and Reflectance of ITO Coated Microsheet

the ITO is strongest in the visible spectrum between 0.35 and 0.75 microns. Since the absorptance of the coated microsheet is equal to 1-T-R, it is evident the increased absorptance of the coated microsheet ( $\alpha = 0.02$ ) occurs primarily in the visible and UV spectrum.

About half of the ITO coated glass tiles were then coated with a back surface reflector. Initial silver depositions ( $1500\text{\AA}$ ) on uncoated microsheet produced coatings with little adhesion and had a tendency to come off under scotch tape test. In order to improve the adhesion of the silver coating to the microsheet, a flash coating of Inconel was deposited by resistive heating vapor deposition to the microsheet and then about  $1500\text{\AA}$  of silver was deposited. The resulting back surface coating provided a high bond strength to the glass. However, that the effect of the Inconel flash coating on the reflectance of the OSR increased the absorptance by about 5 percent therefore no further work was done using the flash coating of Inconel between the glass and the silver. The effect of the  $300\text{\AA}$  of ITO with the back surface coating was to increase the  $\alpha_s$  by about 3 percent which is in agreement with the change observed in the ITO coating on the microsheet without the back surface reflector.

Subsequent coatings of silver on microsheet showed good adhesion if the glass was cleaned prior to deposition. This cleaning was accomplished by wiping the tiles with lens tissue and on occasion preceded with an isopropyl alcohol wash. Also the glass tiles were sputter etched for several minutes before the silver deposition. This cleaning treatment generally provided a surface to which the silver deposition show a strong adhesion.

#### b. OXIDATION

The second set of thin film coatings applied to the polymer films and glass substrates was directed towards examining some of the process parameters in order to improve on the previous results and to determine the reproducibility of the sputtering system. It was found that some initial runs were necessary to precondition the chamber in order to obtain the same highly transparent and conductive coatings deposited previously. Best results were obtained by slowing the deposition rate down to  $1\text{\AA}/\text{sec}$  and using an oxygen/argon gas flow

ratio of about 1/3. This is in contrast to the earlier settings of 2 Å/sec and an O<sub>2</sub>/argon ratio of nearly 1:2. The combination of the slower deposition and reduced oxygen partial pressure gave highly transparent films which were uniformly conductive across the 12 inch square sheets of FEP and Kapton.

The chamber conditioning has been found from this and subsequent depositions to be a significant factor which introduces an indefinite amount of variability in the process parameter optimization. Such a condition will exist in any system which is not dedicated to ITO or IO coating. However, the process parameters which have been identified in this work do provide a starting point at which the necessary parameters can be determined within a few operating cycles of the coating facility.

The effect of the Oxygen/Argon gas flow ratio was varied from 1:3 to 1:4 while maintaining a chamber pressure of 0.5 N/m<sup>2</sup> ( $4 \times 10^{-3}$  mm Hg) during the deposition to determine the effect on the conductivity and the optical properties of the film. In addition, several thicknesses of indium-tin oxide were reactively deposited onto the three types of substrates to evaluate their optical and electrical characteristics.

These oxygen:argon ratios were evaluated using a constant value of the oxygen flow rate of about 8 cc/min into the chamber while maintaining a partial pressure of about 53 mN/m<sup>2</sup> (0.4m Torr). Reactively sputtering at 1 Å/sec, thicknesses of 200Å, 300Å, 500Å, 800Å, 1000Å and 5000Å were deposited during different runs with the deposition time being the only variable. All of the coatings were done with an in situ RF field of about 250 watts applied to the planetary fixture with 30 cm square sheets of FEP Teflon, and Kapton and 12 one inch square tiles of microsheet mounted onto the planetary. Table 2 shows the relative surface resistance of the ITO coatings deposited on the 2.5 cm square (1" x 1") microsheet tiles for the three O<sub>2</sub>/Ar values considered. The resistances were recorded on a digital voltmeter using electrodes touching opposite sides of the 2.5 cm glass squares and averaging over all 12 coated slides. Measurements using a four point probe with a 0.5 cm spacing and a HP 3450A multifunction meter gave values which were typically an order of magnitude lower than those values

Table 2. Surface Resistance of ITO Coated Microsheet\*

DEPOSITION THICKNESS (Å)	OXYGEN/ARGON FLOW RATIO <sup>+</sup>		
	8/24	8/28	8/32
200	530 ± 530	9.1 ± 2.0	
300	1900 ± 1100	6.4 ± 1.1	
500	127 ± 93	2.1	0.7
800	12700 ± 2200 5600 ± 2700	1.3	
1000	735 ± 500	4.0 918G-1*	
5000	70 ± 40	11.2 ± 2.6	

\* Resistances in K  $\Omega$

+ Flow in terms of cc/min

reported in Table 2. There did not appear to be a strong dependence between surface resistance and coating thickness. However, as the partial pressure of oxygen flowing in the system was reduced, a definite increase in coating conductivity was measured, implying less oxidation and creation of a higher concentration of conduction electrons in the film.

While the coating thickness had little effect on coating conductivity, the effect on the optical properties was more pronounced. Figure 6 shows the effect of the coating thickness on the transmittance through the coated microsheet. These values are for the higher resistance coatings in Table 2. Figure 7 shows the same data combined with the coating reflectance to give the dependence of the absorptance on the coating thickness. Table 3 summarizes the

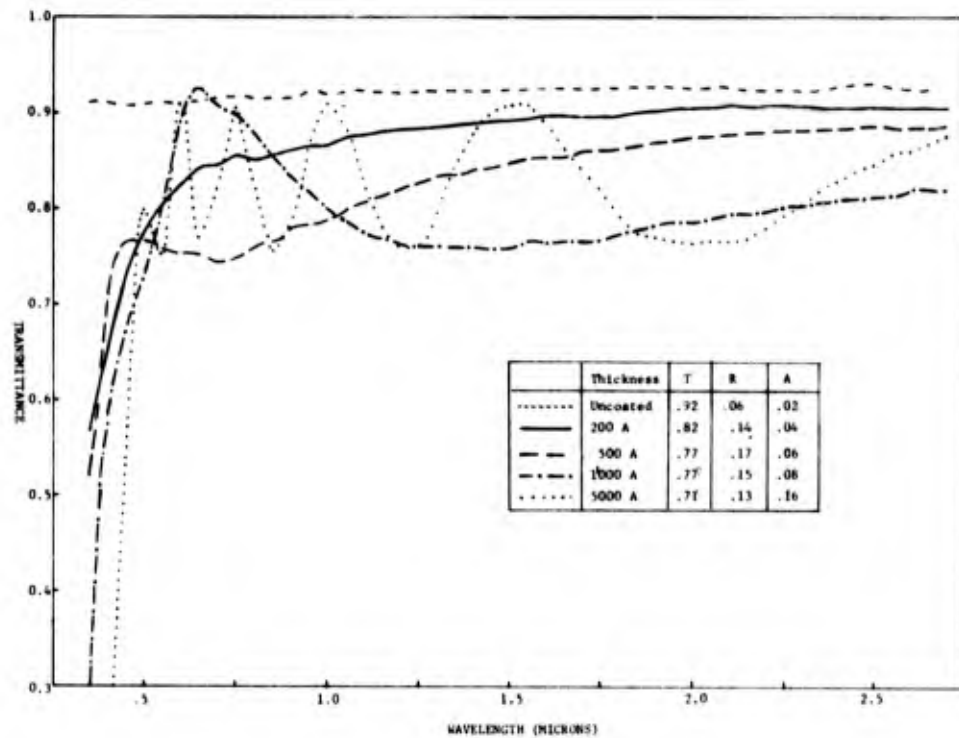


Figure 6. Transmittance of ITO Coated Microsheet

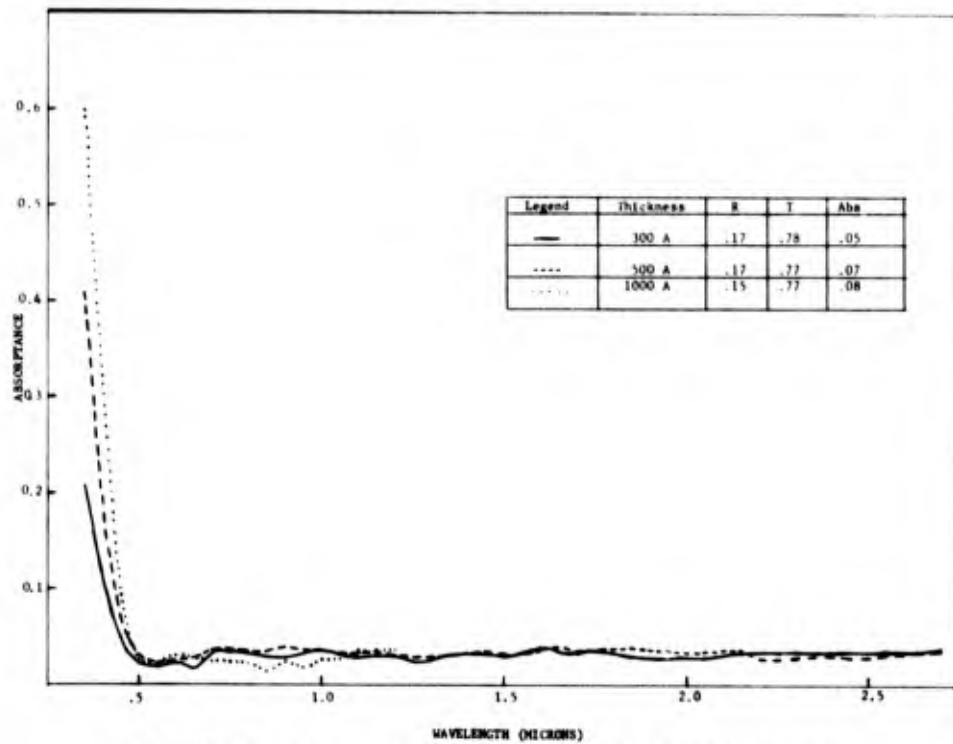


Figure 7. Absorptance of ITO Coated Microsheet

Table 3. Optical Properties of ITO Coated Microsheet

DEPOSITION THICKNESS o (Å)	OXYGEN/ARGON FLOW RATE								
	8/24			8/28			8/32		
	R	T	A	R	T	A	R	T	A
200	.14	.82	.04	.12	.87	.01			
				.15	.84	.01			
300	.17	.78	.05	.18	.80	.02			
				.18	.78	.04			
500	.17	.77	.06	.17	.76	.07	.15	.75	.10
800	.17	.77	.06	.15	.76	.09			
1000	.15	.77	.08	.15	.77	.08			
5000	.13	.71	.16	.14	.71	.15			

transmission and reflectance as a function of the coating thickness and oxygen partial pressure during the sputtering process.

The results of Tables 2 and 3 indicate that while lowering the percentage of oxygen with respect to the carrier gas during the deposition increases the surface conductance of the film, the absorptance of the film is more dependent on the coating thickness. Therefore, a third set of substrates were coated with ITO to further evaluate the effects of the oxygen to argon ratio and to look at coating thicknesses down to 100 Å.

### c. SUBSTRATE

Two sets of ITO coatings were deposited on the three substrates of interest for thicknesses between 100 Å and 500 Å. The two sets were characterized by oxygen:argon flow ratios of 1:3.5 and 1:4 and an oxygen partial pressure typically about 53 mN/m<sup>2</sup> (0.4 m Torr) during the deposition. Table 4 summarizes the order of magnitude surface resistance measurements made immediately following the deposition of the coatings. The measurements were based upon a

Table 4. Preliminary Surface Resistance Measurements of ITO Coated Substrates

SUBSTRATE	THICKNESS	OXYGEN:ARGON FLOW RATIO		
		1:3.5	1:4	
Glass	100 Å	1.5K $\Omega$	0.8K $\Omega$	
		3K	1.0K	
	200 Å	200K	--	
		1K	0.3K	
	300 Å	1K	0.5K	
		--	0.5K	
	500 Å	0.5K	0.3K	
		0.3K	0.3K	
	Kapton	100 Å	0.5K	--
			0.5K	0.3K
		200 Å	0.5K	0.3K
			0.3K	0.2K
300 Å		2M	10K	
		20K	20K	
500 Å		30K		
		10K	4K	
200 Å		10K	200K	
		10K	200K	
300 Å		70K	4K	
		20K	30K	
500 Å	12K			
	150K	10K		
FEP Teflon	100 Å	7K	10K	
			10K	
	200 Å	2M	100K	
		50M	300K	
	300 Å	50M	--	
		30M	500K	
	500 Å	1.0M	500K	
		150K	300K	
	200 Å	400K	200K	
		50K	--	
	500 Å	150K	400K	
		5M	50K	

single resistance measurement of a single substrate made from corner to corner of a one inch glass or 12 inch polymer substrates.

The table shows a definite dependence of the surface resistance on substrate material for a particular operation with the harder substrates such as Corning 0211 microsheet glass having the highest conductive coatings while the coatings on the FEP Teflon consistently had a high surface resistance for all of the thicknesses deposited. It was found that the reactive oxidation of the metal coating could be decreased by increasing the amount of carrier gas in the chamber during the deposition resulting in a decrease of the surface resistance, in some cases by as much as an order of magnitude. There was no observed dependence between the coating thickness and the surface resistance.

These coatings were evaluated to determine the variability between and across samples of similar and dissimilar substrates for the same deposition parameters. Table 5 lists the average of at least 12 measurements at different locations across the 12 inch square polymer substrates or once each for the dozen or so one inch square glass OSR tiles.

The amount of variation observed in the surface resistance of the indium tin oxide coatings on glass was found to be highly dependent upon the coating thickness and independent of the oxygen-argon settings. The typical standard deviations decreased from about 50% of the average value for the 100 Å coatings to about 10% for the 500 Å coatings.

In contrast the standard deviation in the surface resistance of the ITO coatings on the 75 μm (3 mil) Kapton was typically greater than 50% of the average value. Unlike the glass substrate there was no consistent decrease in the variance with the thicker coatings on the Kapton. For the same deposition parameters during the corresponding runs, the indium tin oxide coatings on the FEP teflon substrates showed a large variance in surface resistance in relation to the mean value reported in Table 5. In all cases the standard deviation of measurements across the 12 inch samples was as large as and in some cases up to two times the average of the measured values.

**Table 5. Average Surface Resistance of ITO Coated Substrates\***

Thickness o (Å)	Oxygen: Argon Flow Ratio = 1:35			Oxygen: Argon Flow Ratio = 1:4		
	Glass	Kapton	FEP Teflon	Glass	Kapton	FEP Teflon
100	331	1330	207 x 10 <sup>3</sup>	4.7	292	14.3 x 10 <sup>3</sup>
	59	2960	10 <sup>6</sup>	11.0	65	8.8 x 10 <sup>3</sup>
200	8.5	532	13 x 10 <sup>3</sup>	** (1.1	10	6.7 x 10 <sup>3</sup>
	6.4	492	7.8 x 10 <sup>3</sup>	1.5	31	10.8 x 10 <sup>3</sup>
				2.1	340 *	12.7 x 10 <sup>3</sup> *
300	1.22	134	3.3 x 10 <sup>3</sup>	1.2	26	3.1 x 10 <sup>3</sup>
	0.84	304	2.23 x 10 <sup>3</sup>	1.0	299	2.9 x 10 <sup>3</sup>
500	1.53	633	4.8 x 10 <sup>3</sup>	0.54	8.0	5.4 x 10 <sup>3</sup>
	1.47	88	6.1 x 10 <sup>3</sup>	0.72	5.0	1.5 x 10 <sup>3</sup>

All values reported in KΩ.  
 \*Measured in substorm environment  
 \*\*Sent to AFML

The transmittance and reflectance of the 100 Å, 200 Å and 300 Å indium-tin oxide coatings on the microsheet substrates were also measured for both of the oxygen:argon flow ratios. Table 6 summarizes the measured values averaged over the Johnson curve for the solar energy density spectrum. The absorption is calculated from the measured values of T and R.

Figures 8a and 8b show the reflectance and transmittance for the 200 Å ITO coated microsheet which was deposited at the lower oxygen:argon ratio. This is in comparison to the higher optical absorption through the 200 Å of ITO deposited at the higher O<sub>2</sub>/Ar ratio of 1:3 shown in Figure 6.

**d. REPRODUCIBILITY**

As a result of optical properties and surface resistances of the thin ITO films evaluated above, additional samples of FEP Teflon, Kapton and microsheet were coated with indium tin oxide at the thinner thicknesses. (Deposition #4 of Table 1). These conductive transparent coatings were reactively deposited in the Varian magnetron sputtering unit at about 100 Å thickness. The initial oxygen partial pressure 46 mN/m<sup>2</sup> (0.35 m Torr) was used in combination with a carrier

Table 6. Optical Properties of ITO Coated Microsheet

Thickness o (A)	Oxygen: Argon Flow Ratio=8/28			Oxygen: Argon Flow Ratio=8/32		
	T*	R*	A*	T	R	A
100A	.864	.100	.036	.887	.127	-
200A	.811	.147	.042	.816	.173	.011
300A	.784	.168	.048	.785	.189	.026

\* T = Transmittance

R = Reflectance

A = Absorptance

gas background of about  $0.28 \text{ N/m}^2$  (2m Torr). Using the previously established  $\text{O}_2:\text{Ar}$  ratios at these partial pressures along with the in situ RF activation fairly high resistance coatings, particularly on the FEP were obtained. Surface resistances of about  $2 \times 10^9 \Omega$  per square were measured using a 1.25 cm wide electrode and a 1.25 cm spacing. This is similar to the effect which had been observed earlier. Due to the non dedicated nature of the sputtering unit some chamber conditioning was required to return to the original  $R_s$  and  $\alpha$  properties each time ITO work was resumed following the chamber's use for other applications. In these cases preconditioning did not always return the chamber to the exact state that was present during the previous ITO work. The surface resistance was decreased to  $400 \text{ K}\Omega$  on FEP Teflon by lowering the oxygen partial pressure and subsequently the  $\text{O}_2:\text{Ar}$  ratio while maintaining the RF bias on the planetary at the same power level. About ten consecutive deposition runs were made on 12.5cm (5") square sheets of polymer film to determine the reproducibility of the system and coatings. The average of five surface resistance measurements made on each of the three different type of substrates coated are listed in Table 7. The first three runs were made at the higher oxygen partial pressure and indicate the consistent decrease in

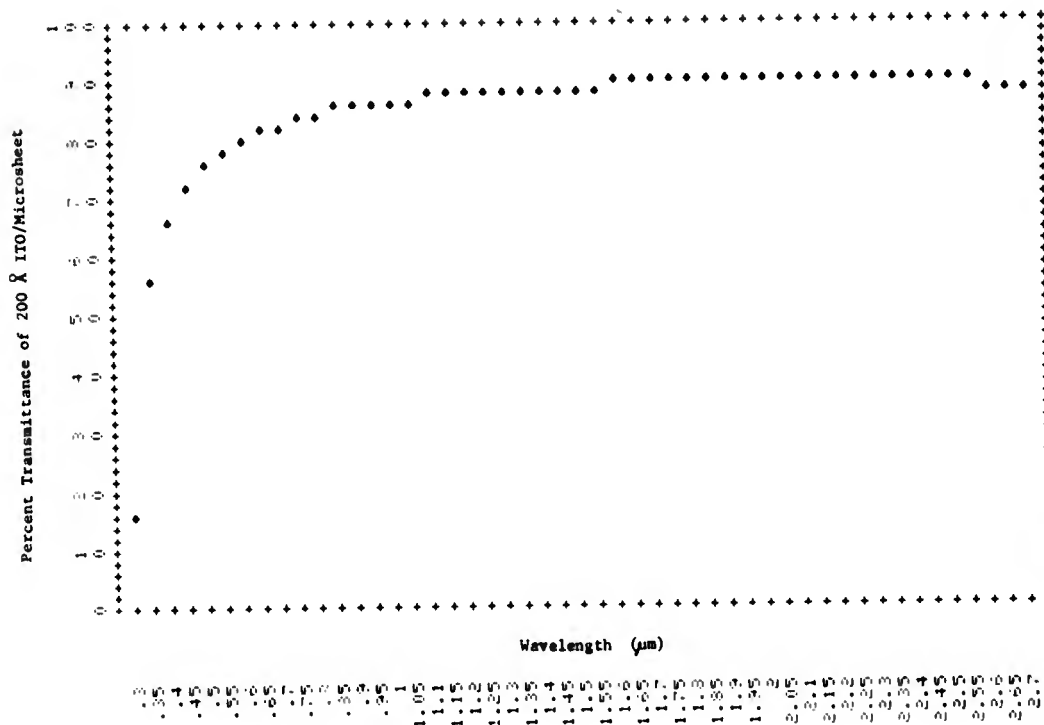


Figure 8a. Percent Transmittance of 200 Å ITO on Microsheet

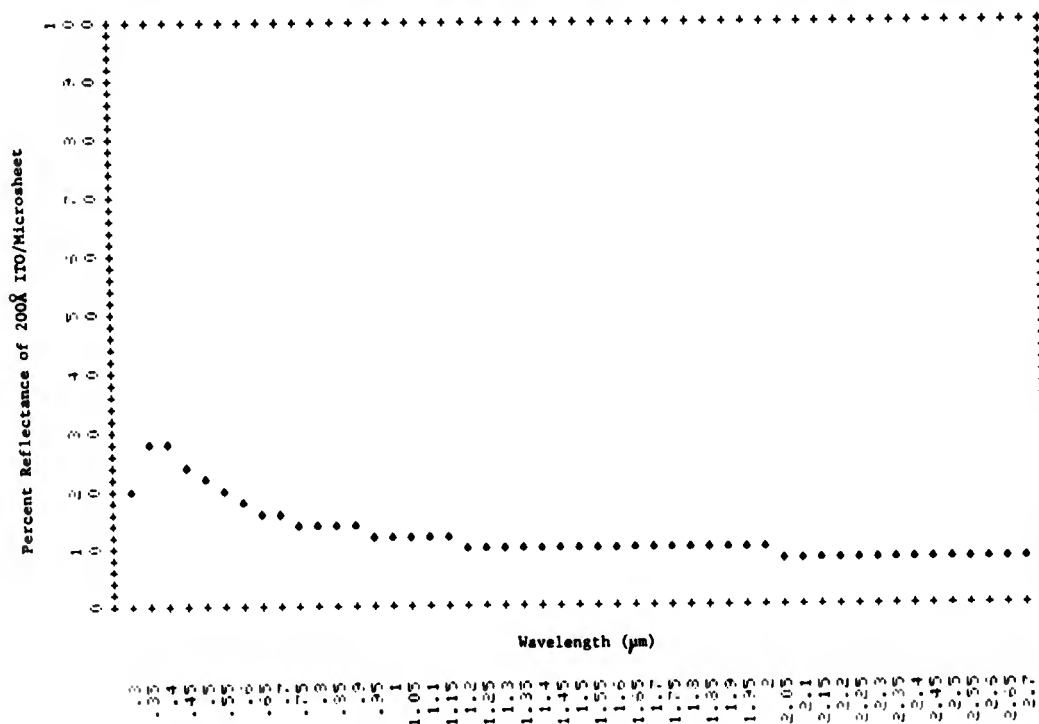


Figure 8b. Percent Reflectance of 200 Å ITO on Microsheet

Table 7. Surface Resistance of 100 Å ITO Coatings

DEPOSITION	SURFACE RESISTANCE (KΩ)		
	FEP TEFLON	KAPTON	MICROSHEET
1	$2 \times 10^5$	200	-
2	$2 \times 10^3$	10	-
3	$5 \times 10^4$	400	-
4	$7 \times 10^3$	80	20
5*	500	25	10
6*	210	6	100
7*	$3 \times 10^4$	90	40
8*	150	3	7
9	460 **	10	-
10	30	0.3	4

\*Back surface metalization deposited after depositing the ITO

\*\* Tested under substorm environment

surface resistance due to the oxygen partial pressure change when compared to the last seven runs. The runs identified as Run 5, 6, 7 and 8 were then back surface coated with 1500 Å of silver in the case of the FEP Teflon and microsheet and 1500 Å of aluminum for the ITO coated Kapton. Measurements of the surface resistance of the ITO coating on FEP Teflon after back surface coating samples 7 and 8 showed nearly an order of magnitude increase in resistance as a result of the silver coating. RF sputter cleaning had been applied to the samples before the silver deposition but it is not definite that this was the cause of the resistance increase.

The surface resistance of the ITO coated FEP Teflon and Kapton samples were remeasured using the same instrumentation and techniques after about four weeks to determine the

stability of the ITO coating conductivity. Table 8 shows the minimum and maximum values of five measurements recorded initially (immediately after deposition) and later (four to five weeks). In all cases the surface resistance had increased and in all but one the increase was by at least an order of magnitude indicating that some additional oxidation had occurred on the polymer coatings during their shelf life. As will be discussed under the materials testing section, the surface resistance of sample number nine was monitored prior to and following electron irradiation to determine if this resistance change is reversible under vacuum.

The reflectance of the four samples of ITO coated FEP Teflon and Kapton which had the back surface reflector coating was measured. Figures 9a and 9b show typical reflectance curves for the 100<sup>o</sup>Å ITO coated silvered Teflon and aluminized Kapton. The average reflectance weighted over the Johnson curve of the solar energy spectrum for both of these curves gave values of  $R = 0.92$  for the FEP Teflon and  $R = 0.68$  for the Kapton. An uncoated silvered FEP Teflon had a reflectance measurement of 0.91 averaged over the same wavelength interval.

#### e. SOLAR CELL COVERGLASSES

The solar cells with the cerium doped coverglasses from PPE have been shown to exhibit charge buildup characteristics similar to uncoated microsheet and fused silica coverglasses<sup>4</sup>. These coverglasses were coated with 300<sup>o</sup> Å ITO during the initial deposition of this program. Figure 10 shows the I-V performance curve of the 2 cm by 4 cm solar cell before and after the 300<sup>o</sup> Å ITO coating was deposited. The curves indicate about a 20% decrease in power at the peak power point (.109 watt to .087 watt) as a result of the coating. A similar decrease shown in Figure 11 was also observed in a 2 x 4 array of solar cells with PPE coverglasses after it was also coated with 300<sup>o</sup> Å of ITO. Since the array had already been fabricated, it was coated in its matrix configuration. The solar cell bus and interconnects between the two sets of four parallel cells were masked during the deposition to prevent shorting the series cells together by the conductive coating. Surface resistance measurements after the deposition showed sheet resistances on all the cells to be of the order of 1000  $\Omega/\square$ .

<sup>4</sup> Transparent Antistatic Satellite Materials, July 1978, AFML-TR-77-174, Part II.

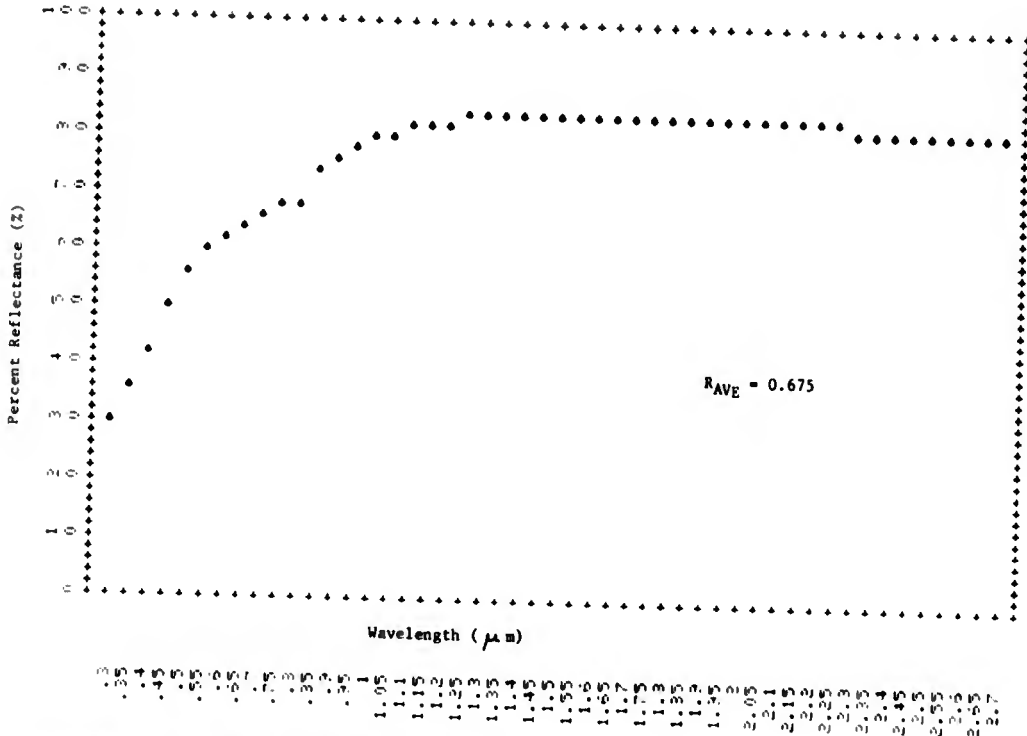


Figure 9a. Percent Reflectance of 100 Å ITO Coated Kapton (Aluminized)

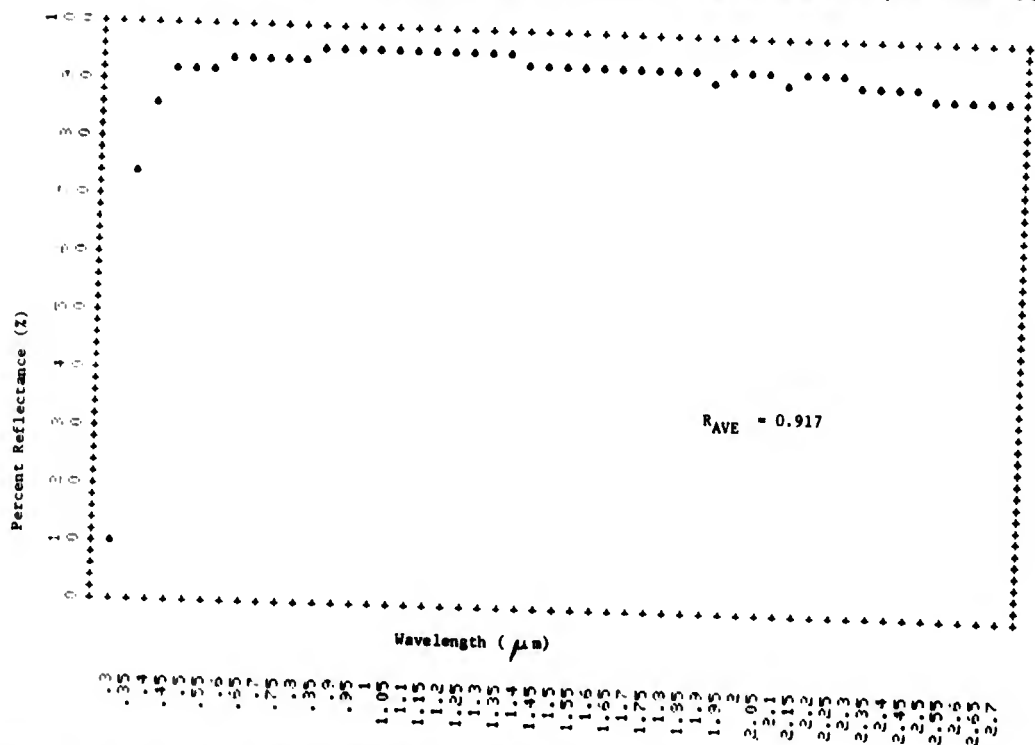


Figure 9b. Percent Reflectance of 100 Å ITO Coated FEP Teflon (Silvered)

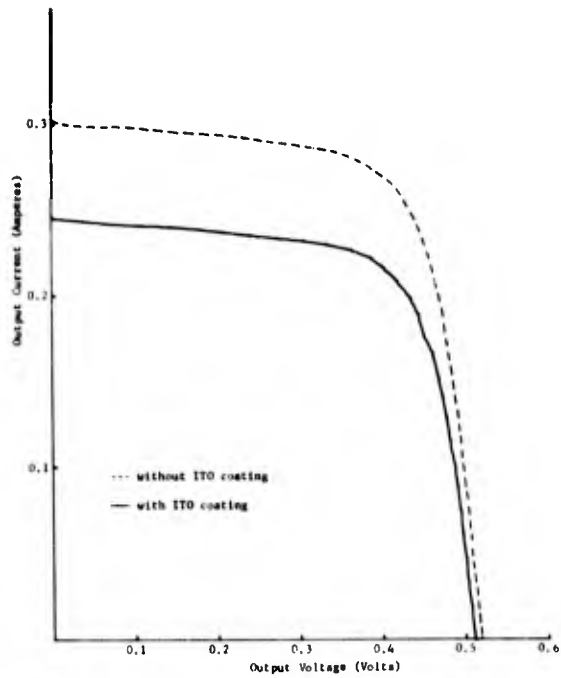


Figure 10. Performance I-V Curve of 2 cm x 4 cm Solar Cell with ITO Coated Ce doped (PPE) Coverglass

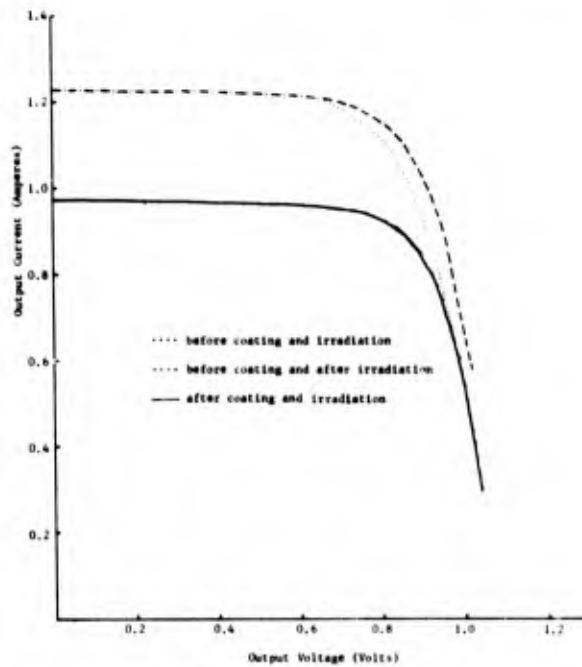


Figure 11. Performance I-V Curves of 2 x 4 Solar Cell Array with ITO Coated Ce Doped (PPE) Coverglasses

Table 8. Temporal Variation of 100 Å ITO Coatings

Deposition	Min. & Max. Surface Resistance (KΩ)			
	FEP Teflon		Kapton	
	Initial	Later*	Initial	Later*
1	---	---	200	60-10 <sup>3</sup>
2	600-5000	10,000-5x10 <sup>5</sup>	10	180-10 <sup>3</sup>
3	50,000	14x10 <sup>4</sup> -20x10 <sup>4</sup>	200-500	600-1.6x10 <sup>3</sup>
4	10 <sup>3</sup> -1.1x10 <sup>4</sup>	10 <sup>3</sup> -4x10 <sup>4</sup>	40-100	100-1000
5	20-2000	2x10 <sup>3</sup> -5x10 <sup>5</sup>	18-30	20-100
6	100-300	5x10 <sup>3</sup> -5x10 <sup>4</sup>	5-7	4-10
7	8x10 <sup>3</sup> -5x10 <sup>4</sup>	3x10 <sup>3</sup> -10 <sup>4</sup>	30-200	4-18
8	100-200	400-2x10 <sup>3</sup>	3	20-40
9	250-600	10 <sup>3</sup> -5x10 <sup>4</sup>	10	150-400
10	30	10 <sup>4</sup> -2x10 <sup>5</sup>	.2-.4	10-30

\*Four to five weeks

In most cases the coating also provided a conductive path from the top of coverglass to the solar cell bus of the order of 40,000 ohms. However, there were some cells for which there was no measurable conductance between the bus and the conductive coating.

Additional glass tiles (OSR's) and solar cell coverglasses were coated with 100 Å of indium tin oxide during deposition 4 of Table 1 to evaluate the performance of solar cells with the thinner more transparent coatings. As a result of previous depositions in the chamber a lower oxygen partial pressure was used and found sufficient to give highly transparent coatings with surface resistances, immediately after deposition, of the order of 20 to 40 KΩ.

The uncoated microsheet coverglasses with a weighted reflectance of 0.11 and a transmittance of 0.880 were bonded to the solar cells with Sylgard 182 and tested in the Large Area Pulsed Solar Simulator (LAPSS) facility. Six cells which exhibited similar performance curves were chosen for ITO coating. In order to determine the effect of coating the top electrode of the solar cell and the variation in coatings between different depositions, the six cells were coated in pairs during three sequential coating operations of the magnetron sputtering chamber. The top electrode of one of the solar cell pairs was masked during the coating to prevent deposition of the oxide onto the electrode surface. A typical coverglass, which was coated with the thin ITO coating, but had not been bonded to a solar cell was measured after the deposition for its reflectance and transmittance. The transmittance of the 100 Å ITO coated coverglass is shown in Figure 12. The weighted average over the solar spectrum was measured at  $R = 0.120$  and  $T = 0.868$  for an absorbance of 0.012 an increase of less than 1% over the uncoated coverglass. Figure 13 shows the IV performance curves of a typical 2 cm by 4 cm solar cell before and after the deposition of the thin conductive coating of indium tin oxide. The curves for the 100 Å ITO coated coverglass indicates about a 2% decrease in power at the peak point (0.115 watt to 0.113 watts). This represents a significant reduction in earlier results. The effect of the coating observed in all of the cells coated was primarily a decrease in the closed circuit current with little to no effect on the open circuit voltage. Furthermore, no differences were observed in the power decreases for those cells whose top electrodes were coated as compared to those cells whose electrodes were not masked during the ITO deposition. This was performed to see if the ITO on the solar cell bus would introduce any significant increase in the resistance of the solar cell circuit.

#### f. OTHER SUBSTRATES

Indium-tin oxides have also been applied successfully to other materials, principally dielectrics used in rf subsystems present on DSCS III which are exposed to the natural environment as a result of their position on the spacecraft. These substrates include copper clad epoxy fiberglass crossover boards and Tefzel spacers in UHF antennas. Stable high resistance coatings of the order of 100K $\Omega$  have been successfully applied to both these materials.

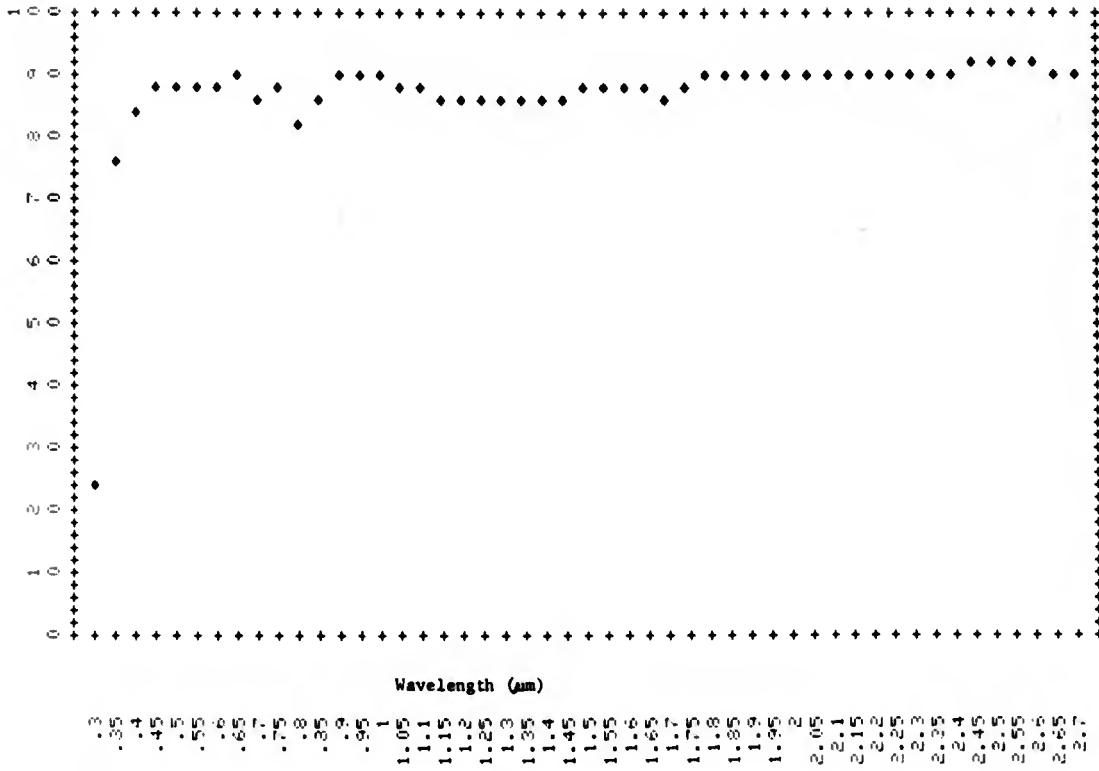


Figure 12. Percent Transmittance of 100 Å ITO Coated Coverglass

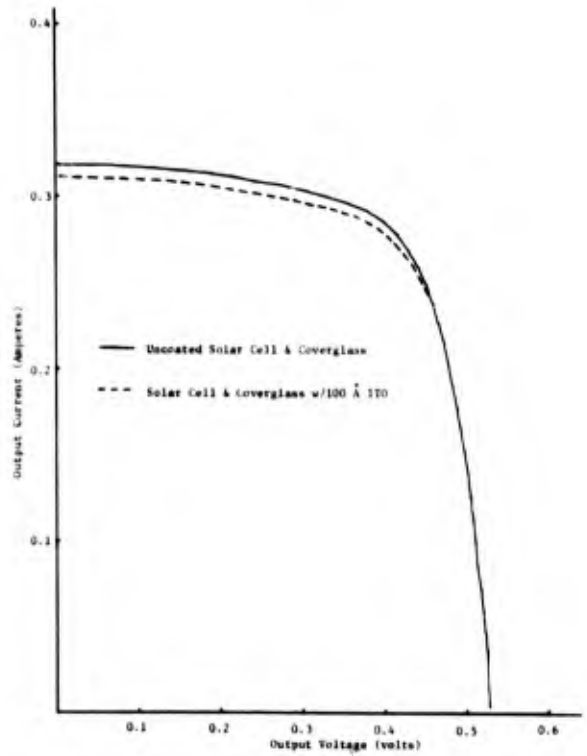


Figure 13. Performance I-V Curve of 2 cm x 4 cm Solar Cell With 100 Å ITO coated Microsheet Coverglass

### 3. INDIUM OXIDE

In addition to indium-tin oxide (ITO) which has been shown to perform well as a transparent conductive coating on the various thermal control and coverglass materials, indium oxide has also shown promise as a highly transparent static charge control coating. Indium oxide (IO) coatings have been deposited by reactive vapor deposition during the previous contractual efforts.<sup>5,6</sup> However, the results of these developmental depositions showed significantly high static surface resistances compared to the deposited by magnetron sputtered ITO coatings. The IO coatings deposited consistently required post deposition heat treatment to improve the transparency of the deposited films. The increased oxidation during this post deposition treatment accounted for the increased transparency as well as the increased surface resistances. This heat treatment also produced the additional undesirable side effect of curling the edges of the polymer substrates particularly the FEP Teflon as a result of the elevated temperatures.

With the introduction of magnetron sputtering using the Varian 3120H S-gun to reactively deposit semiconductor metal oxides onto the substrates of interest it was found that more control of the reactive oxygen environment and argon carrier gas pressure could be obtained while keeping the substrate near room temperatures. The resulting coatings showed considerably less variance between successive depositions as compared to IO coatings deposited using the resistive heating or cathode vapor deposition technique. All of the metal oxide coatings applied by the magnetron sputtering system had used a target of 90% indium and 10% tin while the resistive heating depositions had most success in applying indium oxide coatings. Reactive deposition of ITO from an indium-tin target was not attempted using resistive heating. Therefore it was not clear whether the magnetron sputtering technique was the principal contributing factor to the improved coatings or whether the ITO is basically a better coating than IO.

In order to resolve this difference in the two different coatings applied using different deposition techniques a pure indium target was purchased from Specialty Metals. The indium target was mounted in the magnetron sputtering system in order to reactively deposit indium

<sup>5</sup> Spacecraft Static Charge Control Materials, July 1978, AFML-TR-105, Part II

<sup>6</sup> Transparent Antistatic Satellite Materials, July 1978, AFML-TR-174, Part II

oxide coatings basically under the same conditions that the ITO coatings had been applied. The initial set of coatings were made on microsheet squares using an RF bias on the planetary fixture for predeposition substrate cleaning and during the deposition for improved coating oxidation and stability. These initial coatings were applied in a thickness of about  $500\text{\AA}$  while the argon and oxygen partial pressures and flow rates were varied to obtain a combination of high transparency and low surface resistance. Table 9 summarizes the results of the initial deposits of indium oxide on 2 cm (1") square microsheet tiles. The variation of the argon and oxygen flow rates to obtain conductive transparent coatings was determined by the past history of the chamber as well as the fact that the IO reactive deposition required slightly different values than the previous ITO deposition.

a. DC BIASING

The IO coatings which had been deposited using resistive heating techniques had on occasion used a DC glow discharge before and during the deposition to improve the coatings. Because of the relative ease of using DC biasing techniques as compared to RF biasing a high voltage DC source was connected to the planetary in place of the RF source. This technique has several advantages. It is much easier to use than RF since it doesn't require the sophisticated RF matching networks to insure proper driving of the planetary at the desired power levels. Also such a system does not require the vacuum chamber to be RF tight in order to protect the operator from high radiation fields. Therefore, in designing a scaled-up operation for either magnetron sputtering or resistive heating a DC biased system would be much simpler to design and install and safer to operate.

Thinner indium oxide coatings were next deposited on microsheet, Kapton and FEP Teflon substrates using about 70 watts of DC bias applied to the planetary fixture. Table 10 summarizes the properties of these coatings. These coatings were deposited nearly two weeks after those in Table 9. This is the primary cause for the slight readjustment in the oxygen and argon flow rates reported in Table 10. In order to evaluate the stability of the coatings reported in Tables 9 and 10 their surface resistances were remeasured approximately two weeks after the last deposition, i. e., nearly four weeks after those in Table 9 were deposited. It was found that the surface resistance of both sets of coatings had

Table 9. Properties of Initial 500<sup>0</sup>Å Indium Oxide Coatings Using Magnetron Sputtering

Run #	Substrate	Planetary Bias	Carrier Gas *		Surface Resistance ( $\Omega$ )	Transmittance Comments
			Ar	O <sub>2</sub>		
1	Corning 0211 1"x1"	RF	36	4	160	Very Dark
2	"	"	36	8	500	Medium Dark
3	"	"	30	8	100	Light Gray
4	"	"	28	10	120K	Very Light Gray
5	"	"	28	12	Non Cond.	Very Light Gray
6	"	"	30	11	3K	Very Light Gray

\* Units of flow rate in cc/min

Table 10. Properties of Indium Oxide Coatings using Magnetron Sputtering with D. C. Biasing

Run#	Substrate	Thickness	Carrier Gas *		Surface Resistance ( $\Omega$ )	Transmittance Comments
			Ar	O <sub>2</sub>		
1	Microsheet Kapton FEP Teflon	100 <sup>0</sup> Å	31	11	Non. Cond.	Clear
2	Microsheet Kapton FEP Teflon	100 <sup>0</sup> Å	32	9	18K 14K 30K	Clear
3	Microsheet Kapton FEP Teflon	"	"	"	10K 10-14K 10-30K	Clear
4	Microsheet Kapton FEP Teflon	300 <sup>0</sup> Å	"	"	1K 1K 4-7K	Very Light Tan

\* Units of flow rate in cc/min

changed only slightly. The largest changes were observed in run number four of Table 9 whose surface resistance had increased to  $2.5M\Omega$  and run number two of Table 10 whose resistance had increased to  $600K\Omega$ . Figures 14 and 15 show the transmittance and reflectance of a typical  $100\text{\AA}$  coating on microsheet which is reported in Table 10. The average value of these curves weighted over the Johnson curve of the solar energy density is 0.87 for the transmittance and 0.12 for the reflectance. These values compare well with the values of T and R reported for similar thicknesses of ITO and shown in Figure 12.

#### b. COMPARISON WITH ITO

Several runs were made using the magnetron sputtering system to deposit ITO on the various substrates also using the DC bias on the planetary fixture. Table 11 summarizes the optical and resistance properties of the ITO coatings. These were coated about the same time as those in Table 10. Remeasurement of the surface resistance after two weeks showed considerable change in comparison to the IO coatings. Table 12 compares these changes in the ITO coatings with similar IO coatings reported in Table 10.

Additional substrates of glass and FEP Teflon were then coated with thin coatings of IO and ITO in order to better evaluate the implications that the IO coatings may be more stable than the ITO coatings. The deposition of both oxides were made in thicknesses between  $100\text{\AA}$  and  $300\text{\AA}$  according to the quartz crystal monitor (QCM) which was set to their respective densities. Slightly different argon and oxygen flow rates and partial pressures were used to deposit the IO and ITO coatings. Both coatings were deposited using a DC bias on the sample planetary. It was found that, in general, a slightly higher oxygen flow rate and partial pressure was necessary to deposit coatings of IO compared to the values used to deposit ITO coatings with similar optical and electrical properties. Table 13 summarizes the coatings which were made and their respective surface resistances which were measured immediately after the deposition.

The surface resistance of IO and ITO coatings from selective runs defined in Table V were re-measured about four weeks on the FEP Teflon and glass substrates. Comparison of

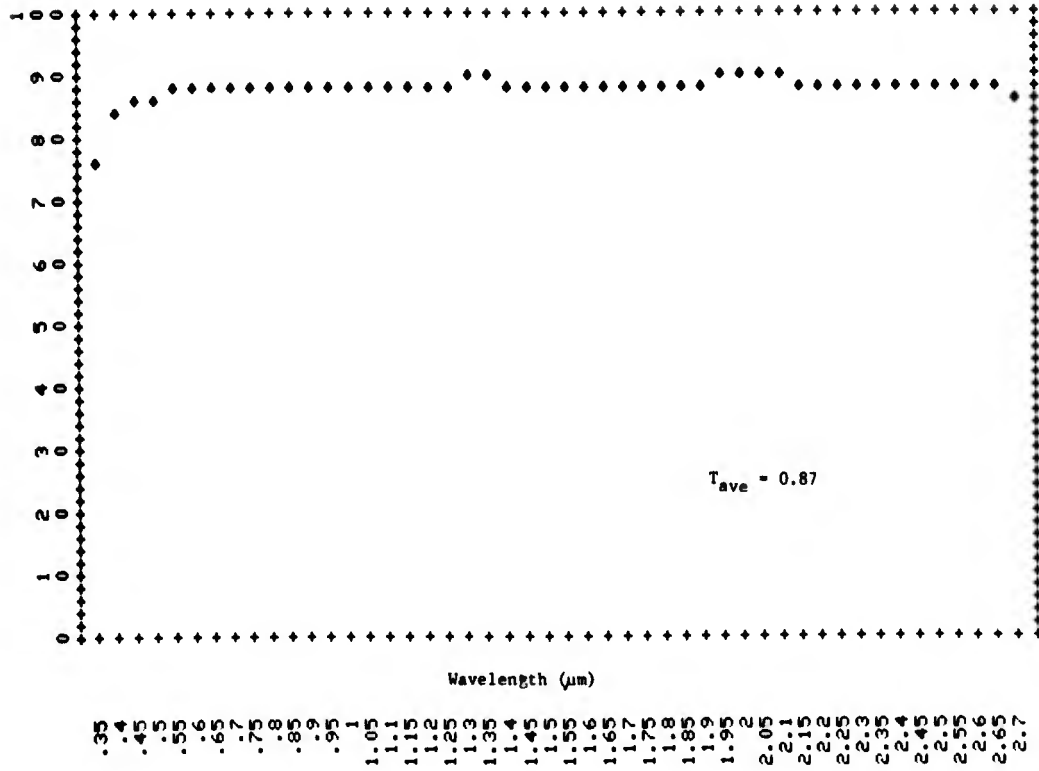


Figure 14. Percent Transmittance of 100Å IO Coated 0211 Microsheet

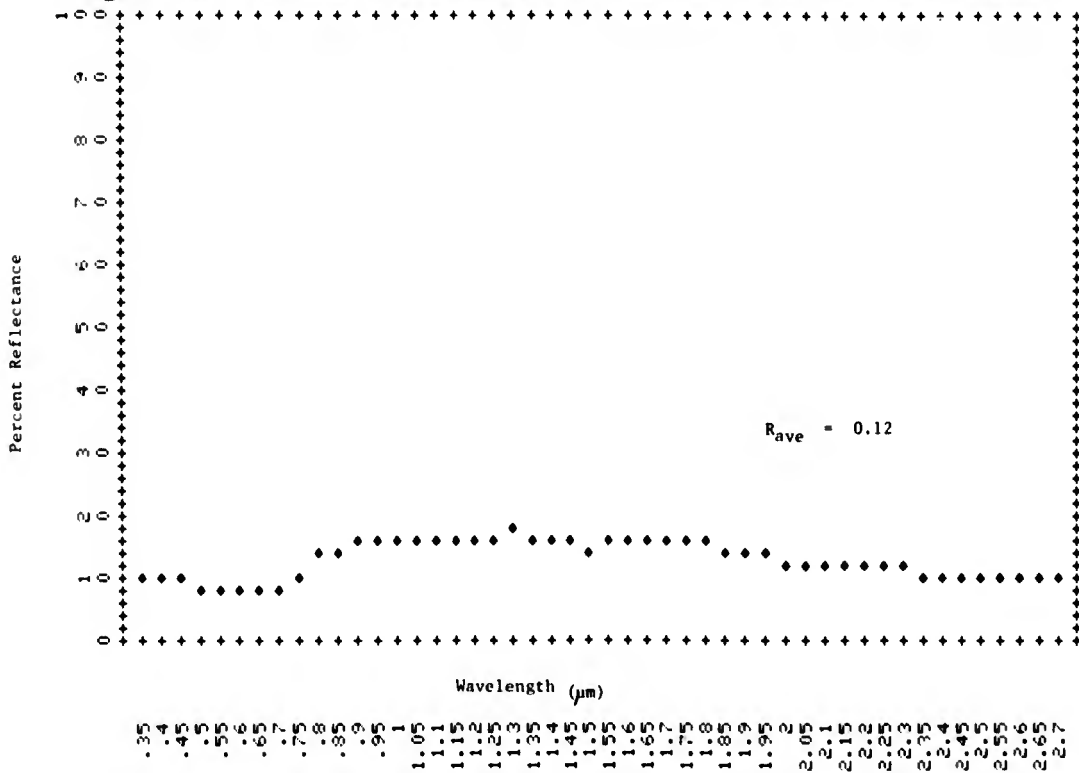


Figure 15. Percent Reflectance of 100Å IO Coated 0211 Microsheet

THIS PAGE IS BEST QUALITY PRACTICABLE  
FROM COPY FURNISHED TO DDC

Table 11. Properties of ITO Coatings Using Magnetron Sputtering with D. C. Biasing

Run #	Substrate	Thickness	Carrier Gas *		Surface Resistance ( $\Omega$ )	Transmittance Comments	
			Argon	O <sub>2</sub>			
1	Microsheet	300Å	30	8	10-20K	Light tan	
	Kapton	"			4K		Clear
	FEP Teflon	"			10K		
2	Microsheet	100Å	30	8	30-40K	Clear	
	Kapton	"			10K		Clear
	FEP Teflon	"			2-5Meg		

♦ Units of flow rate in cc/min

Table 12. Indium Tin Oxide (ITO) and Indium Oxide (IO) with D. C. Biasing

Deposition	Thickness A	Substright	Resistance (As Deposited) ( $\Omega$ )	Resistance (2 Weeks Later) ( $\Omega$ )
ITO	300	Microsheet Kapton FEP	10 - 20K 4K 10K	10 - 20K 700K 200K
ITO	100	Microsheet Kapton FEP	30 - 40K 10K 2 - 5 MEG	5 - 10 MEG 2 - 5 MEG 20 - 50 MEG
IO	300	Microsheet Kapton FEP	1 K 1 K 4 - 7 K	2 K 2 K 16 - 40 K
IO	100	Microsheet Kapton FEP	10 K 10 - 14 K 10 - 30 K	100 K 50 - 100 K 70 - 100 K

**Table 13. Comparison of Conductive Coating Surface Resistance**

<u>SUMMARY OF CONDUCTIVE COATINGS</u>					
<u>RUN #</u>	<u>SUBSTRATE</u>	<u>SIZE (cm x cm)</u>	<u>THICKNESS (Å)</u>	<u>COATING</u>	<u>SURFACE RESISTANCE (Ω)</u>
1	Glass	2.5 x 2.5	100Å	ITO	140 K
	FEP Teflon	2.5 x 5	100Å	ITO	9 Meg
2	FEP Teflon	15 x 15	100Å	ITO	500 K - 5 Meg
3	Glass	2.5 x 2.5	200Å	ITO	20 K - 100 K
	FEP Teflon	2.5 x 5	200Å	ITO	30 K - 40 K
4	FEP Teflon	15 x 15	200Å	ITO	20 K - 80 K
5	Glass	2.5 x 2.5	300Å	ITO	3 - 3.5 K
	FEP Teflon	2.5 x 5	300Å	ITO	5 K
6	FEP Teflon	15 x 15	300Å	ITO	3 - 10 K
7	Glass	2.5 x 2.5	100Å	IO	12 - 18 K
	FEP Teflon	2.5 x 5	100Å	IO	65 - 140 K
8	Glass	2.5 x 2.5	100Å	IO	14 K
	FEP Teflon	2.5 x 5	100Å	IO	80 K
9	FEP Teflon	15 x 15	100Å	IO	35 K - 85 K
10	Glass	2.5 x 2.5	200Å	IO	4 - 6 K
	FEP Teflon	2.5 x 5	200Å	IO	6 - 10 K
	FEP Teflon	15 x 15	200Å	IO	8 - 16 K
11	Glass	2.5 x 2.5	300Å	IO	1.2 K
	FEP Teflon	2.5 x 5	300Å	IO	1.5 K
12	FEP Teflon	15 x 15	300Å	IO	.9 - 1.5 K
13	Glass	2.5 x 2.5	500Å	IO	.5 - .7 K
	FEP Teflon	2.5 x 5	500Å	IO	.4 - .5 K
14	FEP Teflon	2.5 x 5	500Å	IO	.4 - .7 K
15	Glass	2.5 x 2.5	1000Å	IO	.2 - .3 K
	FEP Teflon	2.5 x 5	1000Å	IO	.2 - 1.6 K
16	FEP Teflon	15 x 15	1000Å	IO	.16 - .2 K

measurements of coated samples from run numbers 1, 3, 5, 7, 10, 11, 13 and 15 indicated similar changes in surface resistances for both IO and ITO coatings. In the case of the high resistance ITO coatings (relative to the other values) deposited during runs number 1 and 3 the resistance decreased by factors of 10 and 2 respectively, while for the other IO and ITO coatings the second surface resistance measurements were in general 2 to 3 times higher. Therefore, both coatings seem to have comparable short term shelf life stability with comparable surface resistances for the same coating thickness.

Full 30 cm (12") square sheets of 75  $\mu\text{m}$  Kapton and 12.5  $\mu\text{m}$  thick FEP Teflon were therefore coated with thin films of 100 $\text{\AA}$  of indium oxide for electron irradiation testing. The Kapton and FEP Teflon substrates were coated with IO using an RF bias on the planetary. Following the IO coating the back surface of the Kapton and FEP Teflon substrates were metalized in the magnetron sputterer with about 1500 $\text{\AA}$  of aluminum or silver, respectively. The IO coatings had surface resistances in the 10K  $\Omega/\square$  to 40K  $\Omega/\square$  range before and after the back surface metalization. After about two weeks of open shelf life the surface resistance of the coating on the Kapton and remained about the same while the range of values on the FEP Teflon/indium oxide coating had increased to 20K  $\Omega/\square$  to 400K  $\Omega/\square$ . More uniform coatings were obtained across these substrates than had been previously obtained on 30 cm square samples as a result of taping the substrate to the spherical segment of the planetary rather than using a flat plate holder which had normally been bolted to the rim of the planetary.

#### 4. OXIDE COATING STABILITY

The stability of indium oxide and indium-tin oxide thin films on glass, Kapton and FEP Teflon substrates were evaluated under high humidity and other environmental conditions for extended periods of time. One-inch square OSR tiles of microsheet, and 5 cm (2") square sections of aluminized 75  $\mu\text{m}$  Kapton and silvered 12.5  $\mu\text{m}$  FEP Teflon were coated with thin transparent conductive films of IO and ITO. Both the IO and ITO were coated using approximately the same deposition parameters with a 1 kV DC bias applied for three sets of substrates in coating thicknesses of 100 $\text{\AA}$ , 200 $\text{\AA}$  and 300 $\text{\AA}$ . The six sets of substrates, 3 with IO and 3 with ITO, of varying coating thickness were subjected to these types of environments. In total, five

samples with the same substrate/coating/thickness were made for each of the six sets, one for each of the environments and two control samples.

One group of samples containing all six types of substrates and coatings were suspended over a large container which was partially filled with water as shown in Figure 16, covered and placed in an oven which was maintained at a temperature between +35°C (+77°F) and +44°C (+83°F). A second group of samples were placed in small plastic boxes with holes in front and back as shown in Figure 17 and placed outside the building exposing the samples to a combined environment. The samples were placed in the boxes in order to simplify removal for periodic inspection and measurement, while the holes provided exposure to a confined humidity, temperature and solar environment. A third group of samples containing only the 5 cm by 5 cm coated films were stapled to a board and also placed in the outside environment, along with the second group as shown in Figure 17. This configuration prevented measurement of the optical properties but provided more severe exposure to the combined environment for comparison with the second group of samples while allowing for evaluation of the effects of the exposure in terms of changes in the surface resistance.

Surface resistance and reflectivity measurements were taken on the reference group of samples following deposition of the back surface metalization. For both the indium oxide and indium-tin oxide coatings, the surface resistances were in the range of 1 to 10 k  $\Omega/\square$  with the 300Å coatings having the lower resistances. Figure 18 shows the variation in surface resistance of the reference samples during the month of testing. The reflectivity of each of the metalized substrates of the reference sample group is summarized in Table 14. The measurement uncertainty in these values is  $\pm 1\%$ .

Table 14 shows the reflectivity values of the test samples after 3 days of environmental testing. The samples which were suspended in the container above the water showed about 1-2% change in reflectivity as a result of the elevated temperature (35-40°C) and humidity. However, it was observed when these samples were retrieved from the oven that the cover had not been placed

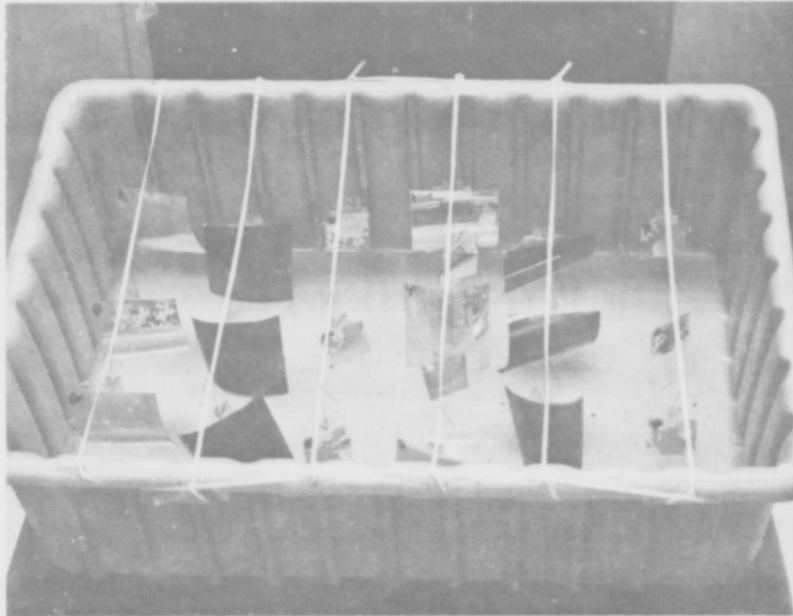


Figure 16a. Humidity Test Set Up (Top View)

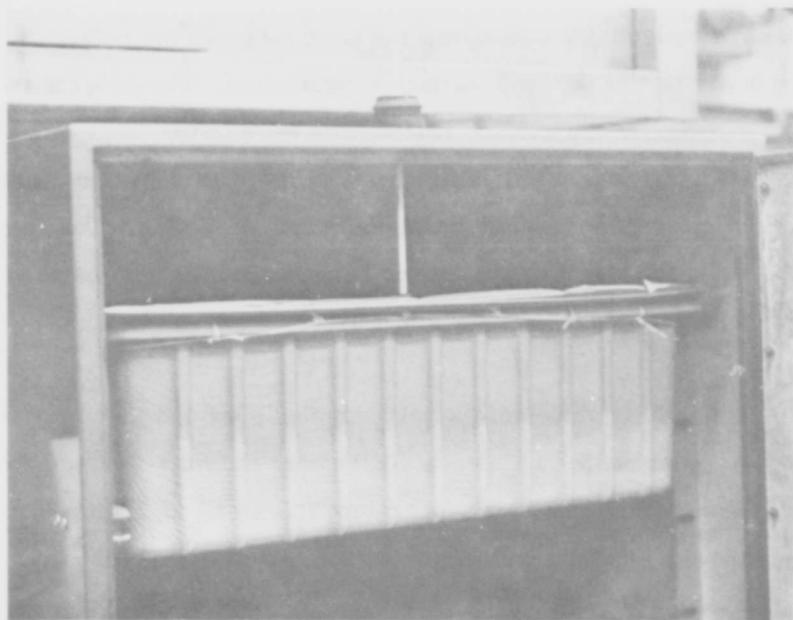


Figure 16b. Humidity Test Set Up (Side View)



Figure 17a. Combined Exposure Test Set Up (Close-Up View)

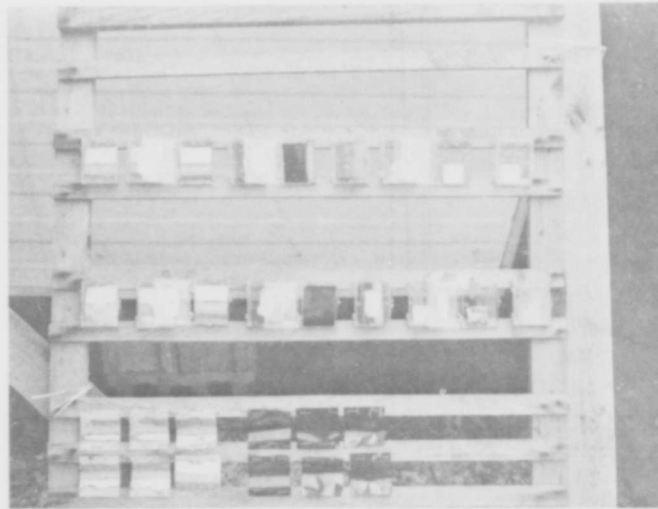


Figure 17b. Combined Exposure Test Set Up (Total View)

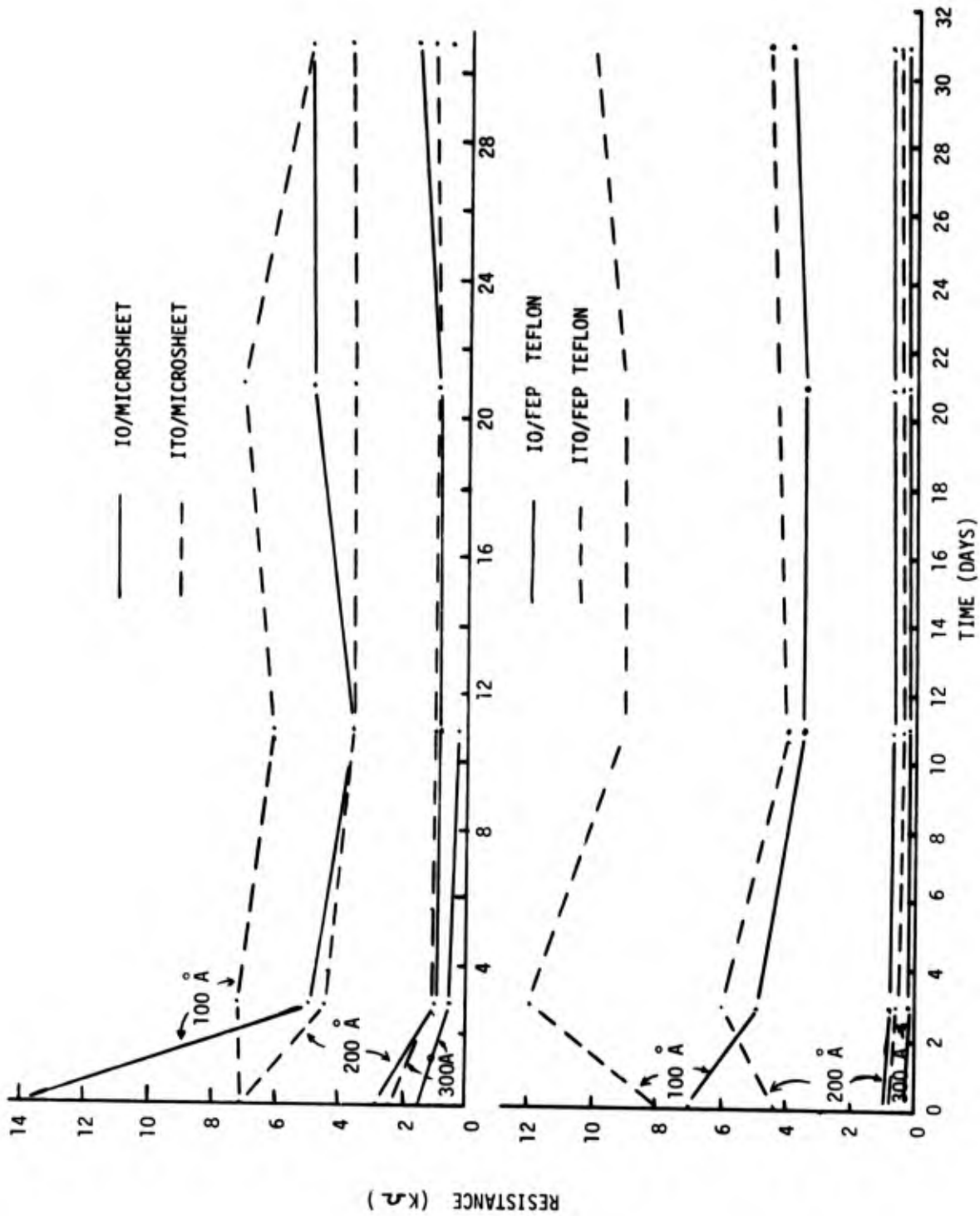


Figure 18a. Surface Resistance Stability of Reference Samples

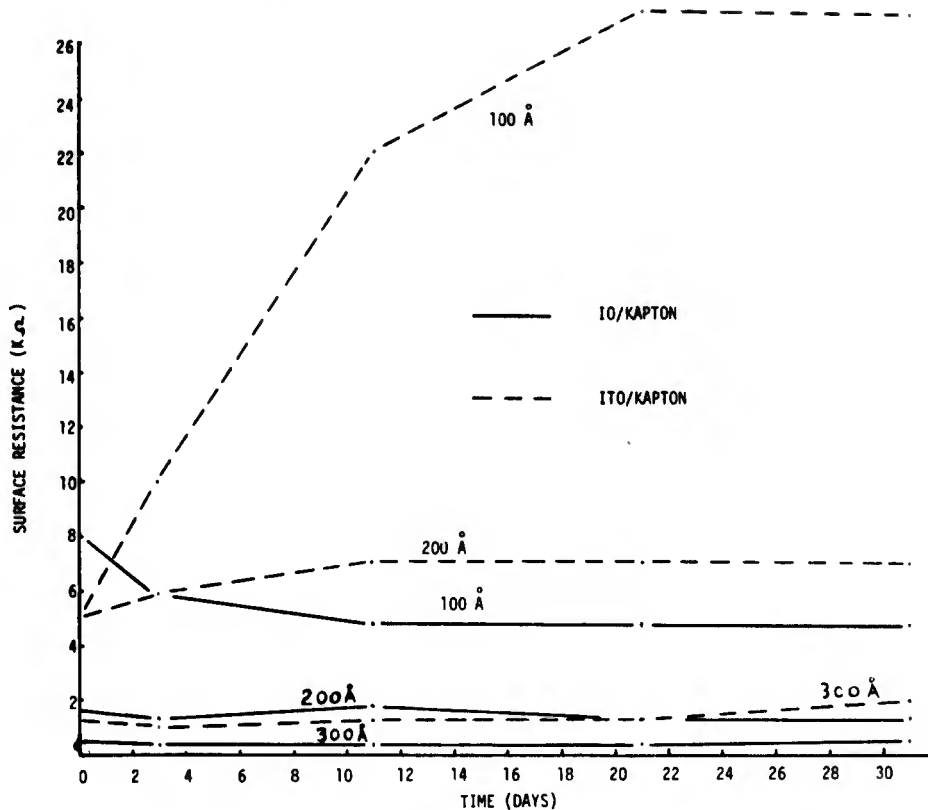


Figure 18b. Surface Resistance Stability of Kapton Reference Samples

over the container in order to maintain a high humidity. A second group of reference samples was substituted in the humidity test container. The reflectivity of the second group of reference samples was measured after the samples had been in the humidity environment for 13 days. The results are plotted in Figure 19. Further measurements of the reflectivity was not possible because of peeling and flaking in the silver backing on the glass and FEP Teflon samples.

The surface resistance of the initial set of samples in the humidity test was monitored for nearly three weeks before the samples and container lid was replaced. Figure 20 includes both sets of data for the two experimental set ups. The first set covers the first 21 days while the second set covers the final 13 days with the glass cover. The curves indicate the large increase in the 100Å coatings compared to the 200Å and 300Å thickness and larger variation in the ITO versus the IO coatings.

Table 14. Preliminary Environmental Results

Coating	Substrate	Coating Thickness (Å)	REFLECTIVITY		3 Days (Exposure)	
			Initial	3 Days of Humidity		
ITO	Glass/Ag	0	0.92	-	-	
		100	0.90	0.88	0.83	
		200	0.88	-	-	
	FEP/Ag	300	0.86	0.84	0.82	
		0	0.86	-	-	
		100	0.86	0.85	0.85	
	Kapton/Al	200	0.82	-	-	
		300	0.80	0.82	0.81	
		0	0.37	-	-	
	IO	Glass/Ag	100	0.37	-	-
			200	0.37	-	-
			300	0.35	-	-
FEP/Ag		0	0.92	-	-	
		100	0.86	0.85	0.81	
		200	0.84	-	-	
Kapton/Al		300	0.81	0.79	0.76	
		0	0.86	-	-	
		100	0.81	0.82	0.84	
IO	FEP/Ag	200	0.78	-	-	
		300	0.76	0.76	0.78	
		0	0.37	-	-	
	Kapton/Al	100	0.37	-	-	
		200	0.34	-	-	
		300	0.29	-	-	

Figure 20 shows a typical variation in the coatings on all three substrates. The behavior in the coating surface resistance as a result of the higher temperature and humidity was found to be dependent upon coating thickness and independent of the substrate. The curves indicate a large increase in the 100Å coating compared to a high stability in the 200Å and 300Å thicknesses. The ITO also exhibited much larger variations than the IO coatings. However, the variation in surface resistance during the two to three week exposure of all the coatings were well within the allowable range for charge control surface properties.

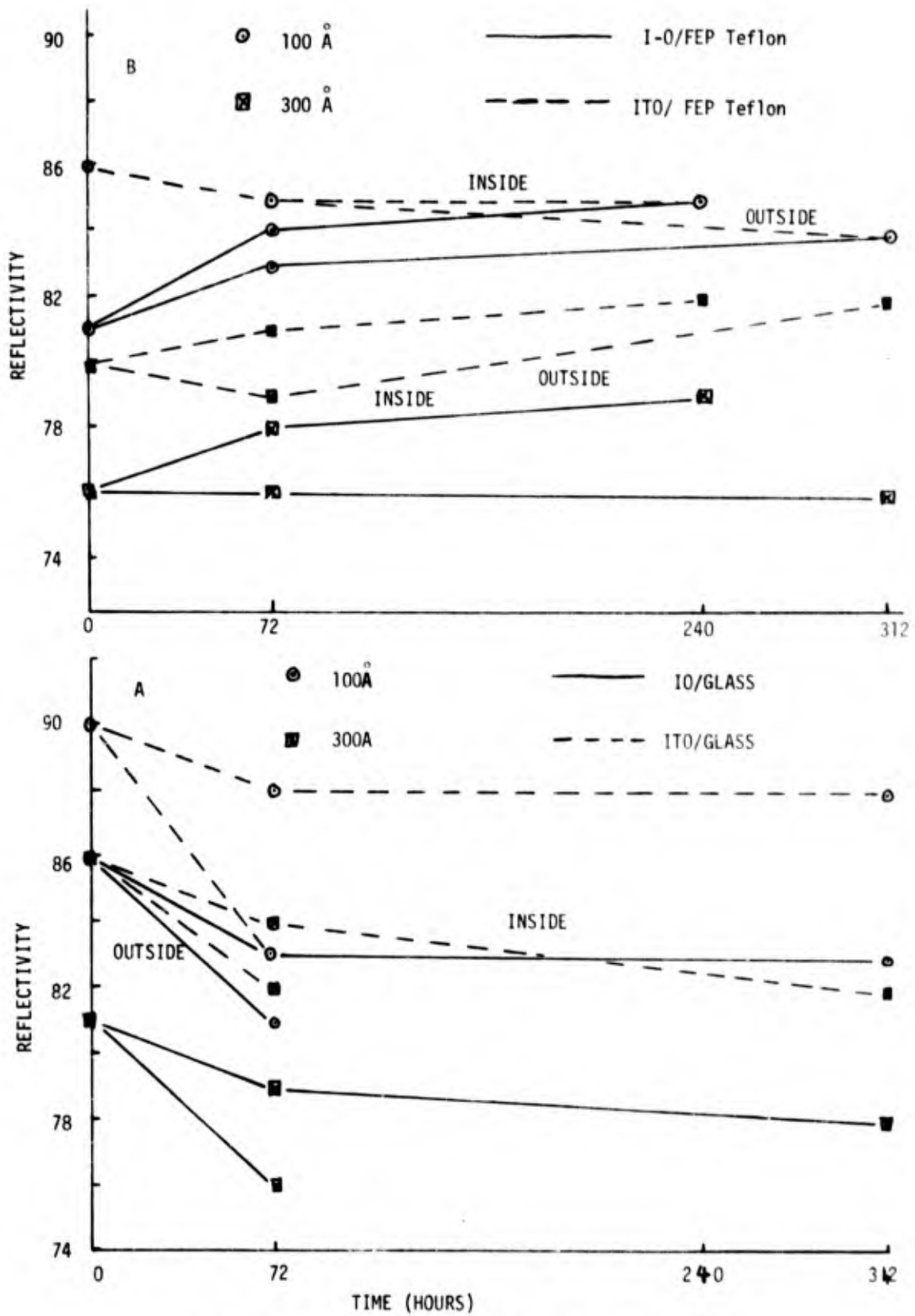


Figure 19. Solar Reflectance During Humidity Test

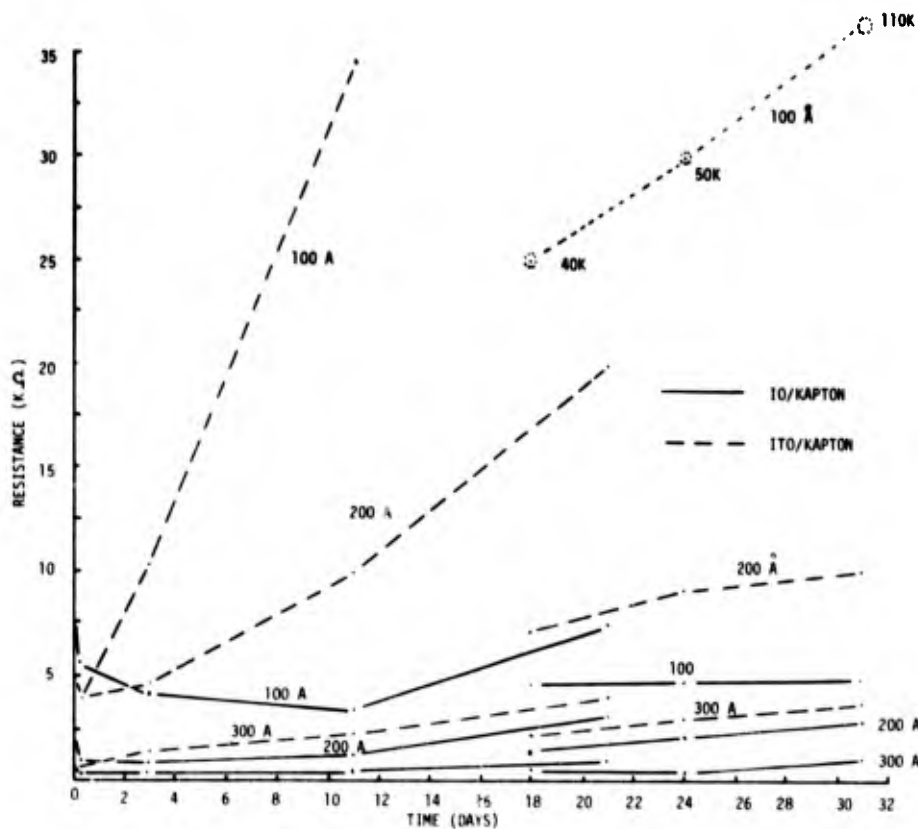


Figure 20. Typical Surface Resistance Variation During Humidity Test (Kapton)

Also included in Table 14 are the results of initial reflectivity measurements on samples exposed to the combined environment while enclosed in the ventilated boxes. Additional measurements of the reflectivity was not possible due to peeling and flaking of the back surface coating. Surface resistance measurements initially made on these samples indicated an increase in surface resistance which was consistently less than an order of magnitude. The greatest changes were observed in the  $100\text{\AA}$  thick coating on all the substrates. The measurements were made using a VOM with a range of  $10^7 \Omega$  using 1.25 cm wide copper tape tabs spaced on the surface about 1.25 cm. The measurements were continued for a month. Figures 21 and 22 show the typical behavior of the coatings during this exposure.

In general the  $100\text{\AA}$  coatings of both oxides had increased above  $10^7$  ohms/ $\square$  after 30 days of exposure. Obviously the thicker coatings are more stable. Also as would be expected the

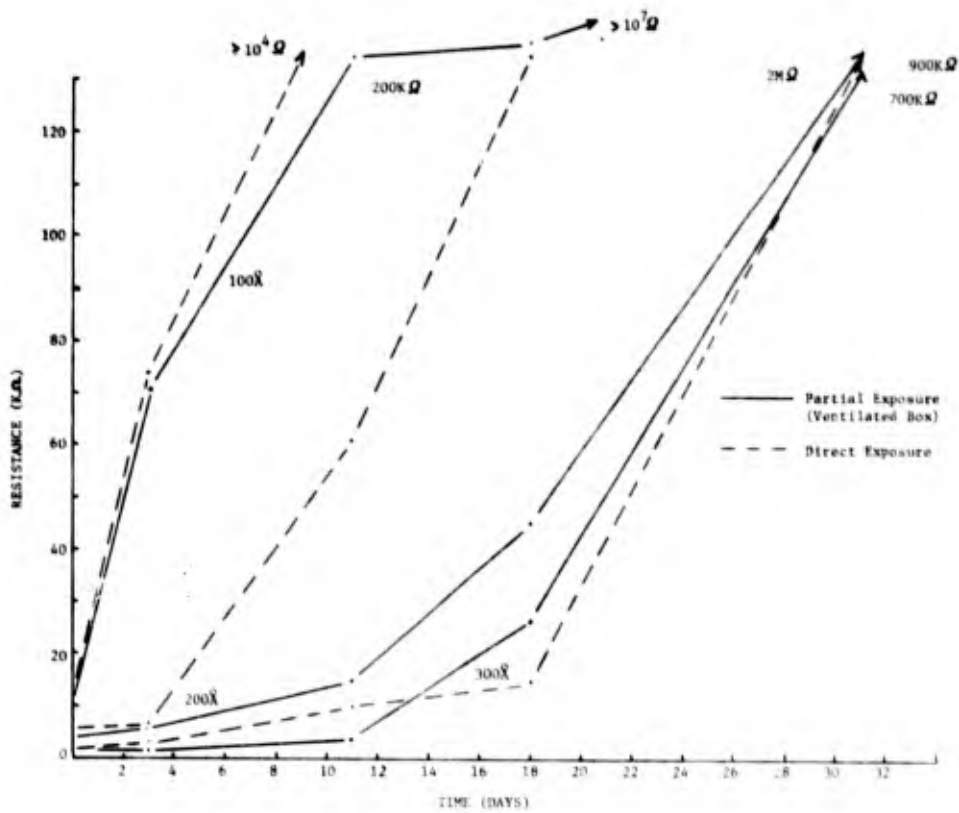


Figure 21. Environmental Stability to Combined Environment Exposure (ITO/Kapton)

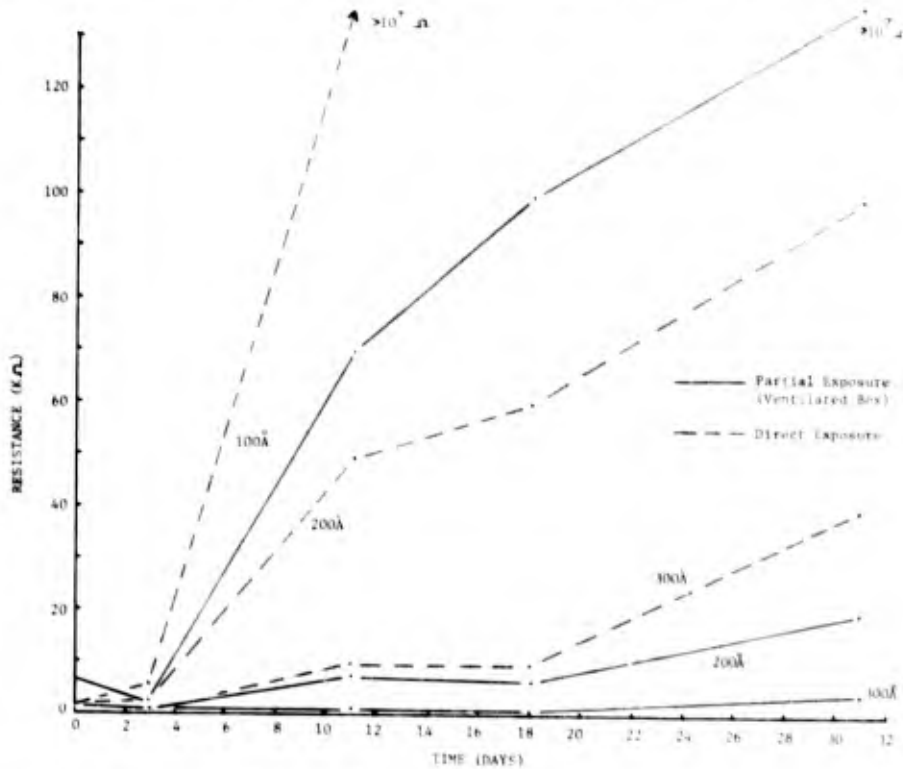


Figure 22. Environmental Stability to Combined Environment Exposure (I/O Kapton)

degradation to those samples mounted inside the ventilated boxes is less severe than those exposed directly to the elements. The indium oxide coating seems to have a more stable surface resistance than the indium-tin oxide for comparable coating thicknesses.

##### 5. COATING ADHESION

The indium oxide and indium-tin oxide coatings which have been reactively deposited by magnetron sputtering using an RF or DC bias on the planetary have, in general, been relatively stable in their optical and electrical properties when held in a controlled environment. Surface resistance measurements over a period of weeks have shown some changes to the resistance typically less than an order of magnitude or slightly larger for the thinner coatings but the changes have always been well within acceptable limits for successful charge control. No significant changes have been observed in the optical transmittance of the films over the same period of time based on visual inspection of the films during this time. Relatively hard coatings have been routinely obtained on the glass and Kapton substrates. The hardness of the coatings in these cases are measured by the coating's surface resistance stability under scotch tape and Q-Tip rubbing tests. In general, very small changes, if any, have been observed in the surface resistance of either indium oxide or indium-tin oxide coatings on glass and 75  $\mu\text{m}$  thick Kapton as a result of tape and rubbing tests. On the other hand, changes in the surface resistance of thin IO and ITO coatings on FEP Teflon have been observed to be quite high as a result of the tape test and in the case of the rub test using a Q-Tip, the conductivity has in some cases been lost entirely. A related behavior of the adhesion or strength of the conductive coatings on FEP Teflon had been observed last year in our attempts to find a suitable bonding technique for attaching grounding tabs to the ITO coated surface.<sup>7</sup> In order to improve the surface adhesion or strength of the conductive coating on FEP Teflon and to obtain coatings with more resistance to rubbing, several intermediate ultra-thin surface coatings were applied to 125  $\mu\text{m}$  FEP Teflon films before application to the indium oxide coatings.

---

<sup>7</sup>Spacecraft Static Charge Control Materials, July 1978, AFML-TR-77-105 Part II pg 27.

This series of experiments involved evaluation of application of flash coatings, approximately  $50\text{\AA}$ , of chromium, reactively deposited chromium and oxygen, the reactive deposition of aluminum and oxygen and the predeposition etching of the substrate. Although interest was primarily in the FEP Teflon surface behavior, 2.5 cm square glass tiles and 5 cm x 5 cm films of  $12.5\ \mu\text{m}$  FEP Teflon were coated with the surface conditioning coatings and indium oxide. Typical  $200\text{\AA}$  of indium oxide was reactively deposited on top of the flash coated surfaces using either a DC voltage of 1 kV or about 70 watts of RF power applied to the planetary during the IO deposition. The following observations were made from tape and Q-Tip rubbing tests on the IO coatings before and after deposition of the back surface metalization.

1. The aluminum oxide was highly transparent.
2. The chrome coatings developed a yellowish or tarnished appearance after back surface etching.
3. The chrome oxide was fairly dark even at  $50\text{\AA}$ .
4. The surface resistance of the IO on the FEP Teflon typically increased by a factor of about 3 for all surface flash coatings after the tape test.
5. The IO surface resistance increased above  $10^{12}$  ohms after Q-Tip rubbing test on the chrome and chrome oxide coated samples.
6. The IO coating with the aluminum oxide undercoating failed the Q-Tip test when it was applied with a DC bias to the planetary but passed when an RF bias was used during the deposition.
7. The IO coating applied with an RF bias failed the Q-Tip rub test after an RF etch was used to clean the back surface for silver coating.

#### 6. SILICA NITRIDE

Silica nitride coatings were applied to 2 cm x 4 cm 0211 coverglasses to evaluate their charge control behavior. The coatings were reactively deposited by RF sputtering in an MRC model 8500 RF Sputtering Unit from a silicon target in a nitrogen atmosphere. The surface resistance of the coatings on a 5 cm by 7.6 cm glass slide was in the mid  $10^{14}$  ohms range using a Hewlett Packard Model 4329A high resistance meter. Figure 23 shows a plot of the transmittance and reflectance of the coating on the 0211 coverglass.

The coating thickness was measured at about  $750\text{\AA}$ . The following table shows the results of additional measurements on the coated and uncoated substrates. As with the other optical measurements, the uncertainty is about  $\pm 1\%$ .

Substrate	<u>Uncoated</u>		<u>Silica Nitride</u>	
	R	T	R	T
$\text{SiO}_2$	0.11	0.87	0.07	0.93
Microsheet	0.12	0.80	0.10	0.90

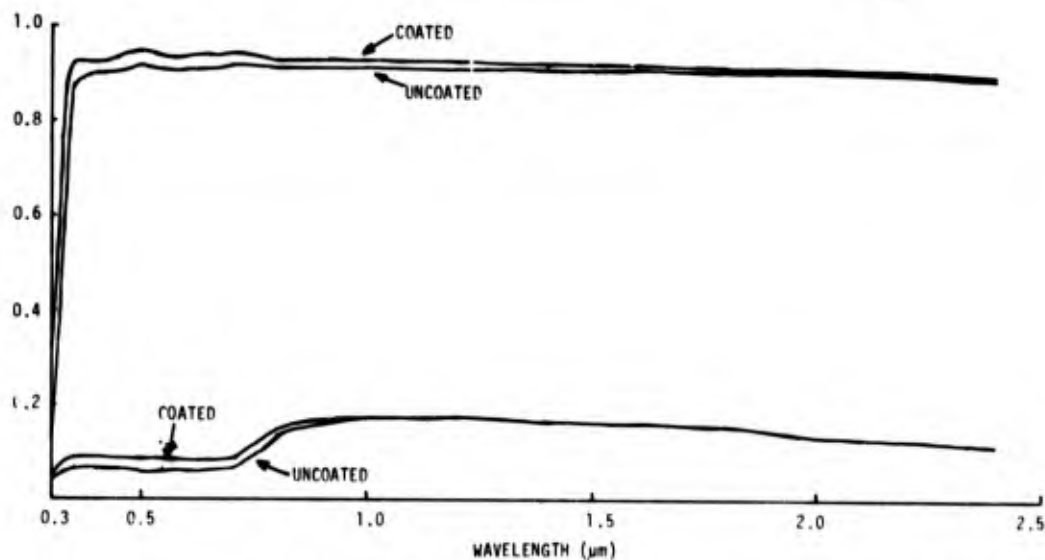


Figure 23. Transmittance and Reflectance of  $\text{Si}_3\text{N}_4$  on Microsheet

## 7. CONDUCTIVE GLASS DEVELOPMENT

Development of conductive lithium lanthanum borosilicate glass tiles was resumed from the previous contract efforts with emphasis in using a process typically required for economical production of ribbon glass as opposed to the previously used process of cutting and polishing from solid blocks of glass. Initial results produced glass ribbons of the conductive glass which were about 1.25 cm wide and about 15 cm long. It was anticipated that minor refinements in the drawing apparatus and annealing more quickly at the correct temperature would produce 5 cm wide glass ribbons about 50 cm long which could be cut into appropriate size tiles for OSR and coverglass applications.

During the process, the GE-1TL, a lithium lanthanum borosilicate glass modified with  $\text{CeO}_2$ ,  $\text{Ta}_2\text{O}_5$  and  $\text{ZnO}$ , was heated in a crucible to about  $950^\circ\text{C}$  at which temperature the glass

became very fluid. Ribbons of the glass were then formed by pouring the melt through a pair of rotating steel rolls shown in Figures 24a and b. The ribbon formed in this manner was between  $330\ \mu\text{m}$  and  $380\ \mu\text{m}$  thick. Initial ribbons were only about 1.25 cm wide, but after adjusting the speed and tension on the rollers, the ribbon width was increased to about 5 cm with lengths formed up to 20 cm in the gravity feed apparatus. Following the drawing process, the resultant ribbon must be annealed to remove residual stresses which occur because of the rapid cooling of the glass during the drawing process. This was accomplished by a heating cycle of about  $450^{\circ}\text{C}$  for one hour, followed by slow cooling to room temperature.

Ribbon, thus formed, has been cut into roughly 2.5 cm squares. At present, the ribbon, after annealing, is not perfectly flat with typical variations in the height of about 1mm for one inch squares when laid on a flat surface. Measurement of the total reflectance and transmittance of the  $330\ \mu$  thick 2.5 cm square tiles have a value of  $R = 0.13$  and  $T = 0.83$ , when averaged over the air mass zero Johnson Curve. This gives a value of about 0.03 for the solar absorptance. The glass as measured had rough surfaces on both sides since it could not be polished with the present variations in height.

Additional ribbon forming work is necessary to develop sufficient skill to make ribbon which is more flat than the current material. Surface tension, even during the rapid cooling of ribbon formation, tends to curl the edges of the ribbon. Additional heat treating methods are being investigated in an effort to overcome this undesirable behavior. The approach is to determine the temperature on the thermal expansion curve, shown in Figure 25, where the glass will relax under its own weight, but not flow sufficiently to adhere to the stainless steel plate its laying on.

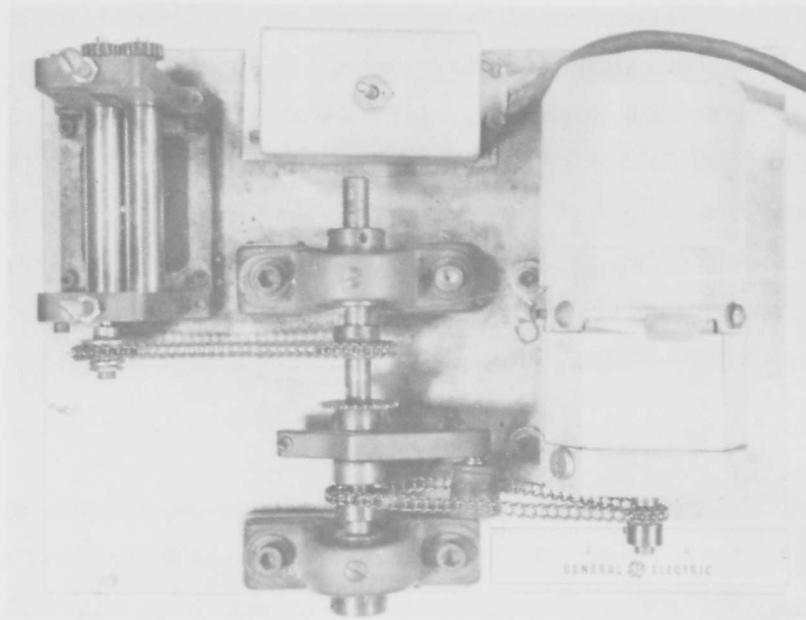


Figure 24a. Ribbon Forming Set Up (Top View)

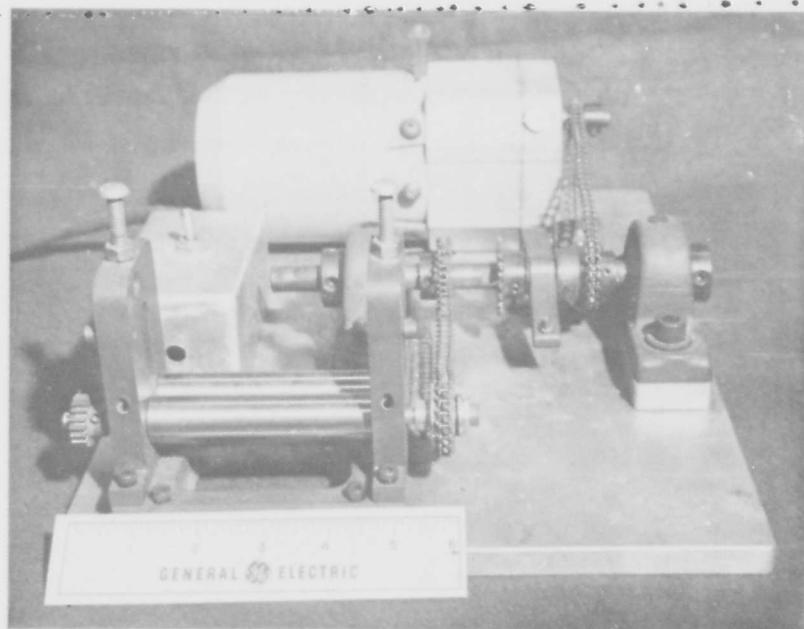


Figure 24b. Ribbon Forming Set Up (Side View)

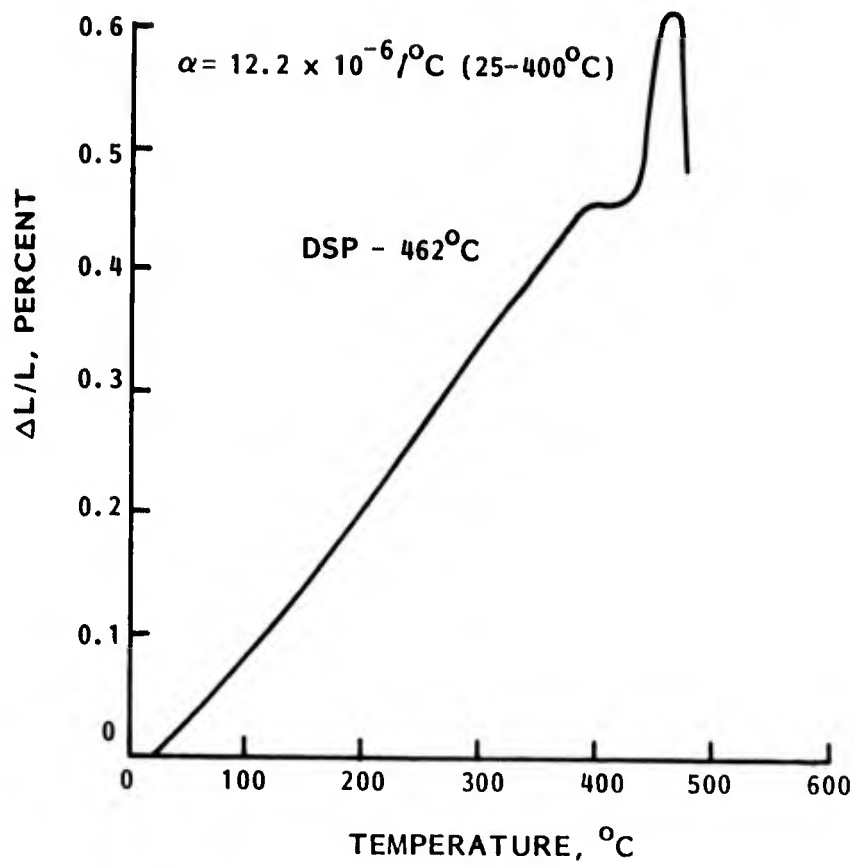


Figure 25. Thermal Expansion of GE-1TL

SECTION III  
MATERIALS TESTING

1. INTRODUCTION

The materials testing discussed in this section describe the evaluation of the IO and ITO coated polymers under electron irradiation simulating a geosynchronous electron plasma environment. The optical and electrical characterization of the individual depositions were performed as required to judge the progress of the process and materials development and therefore has been reported as part of the previous section.

The initial phase of electron irradiation measurements were made in the small ESD characterization facility shown schematically in Figure 26. This facility was used to evaluate the vacuum stability of 11 cm diameter conductive transparent coated samples and the surface resistance before and after electron irradiation for a particular ground bonding.

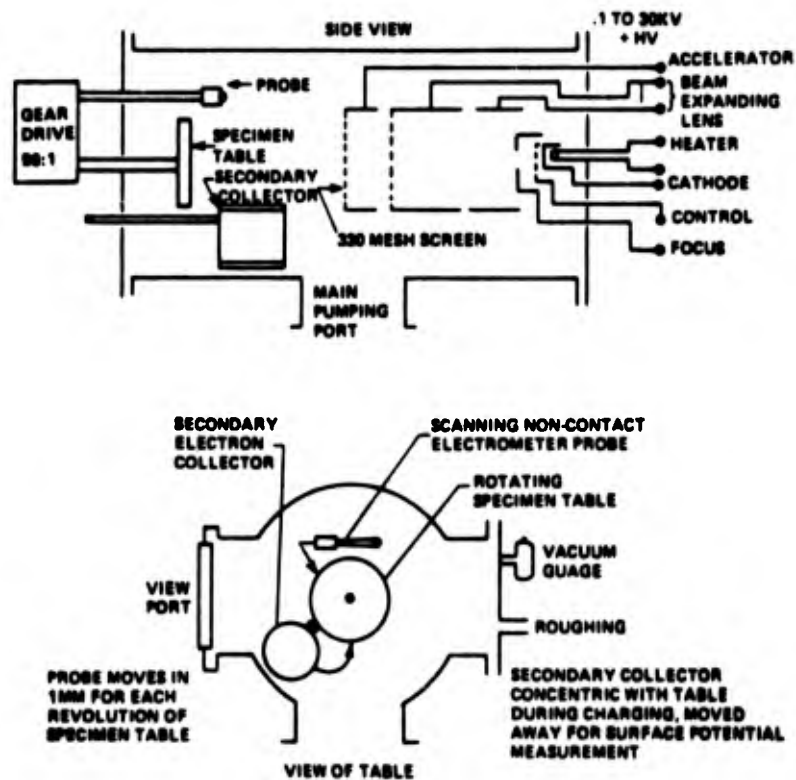


Figure 26. Functional Diagram of ESD Test Facility

The electron flood gun was designed to provide a typical geosynchronous electron substorm environment with electron energies between 0.5 and 20 keV and current densities averaged between 0.5 and 5.0 nanoamperes/cm<sup>2</sup> for a period of several hours. The diagnostic assembly consists of an electrically isolated table for holding specimens up to 11.5 cm in diameter. The specimen table is grounded through a Keithley 610 electrometer used in a current measuring mode. By measuring the current flowing through the table the diffusion current through the specimen or any displacement currents generated by material surface charge buildup was monitored. A Monroe electrostatic non-contacting surface potential probe was mounted to a movable arm which is connected through a gear box to a DC reversible electric motor. The motor was coupled to a resistance commutator for driving one axis of an XY recorder while recording surface potentials. The arm movement allowed the probe to be swept across the sample before, during and after irradiation or to be swung completely out of the electron beam so that it would not shadow or interact with sample during the irradiation. A secondary electron collector cylinder was also part of the assembly which was swung in place around the sample during the charging phase. It was also used to monitor charged particles leaving the surface of the sample during an ESD. The cylinder was swung away from the sample when the surface potential probe was being used.

#### a. LARGE AREA TEST FACILITY

Since the above facility was capable of evaluating samples up to 11.5 centimeters only a new irradiation facility was assembled to measure the response of the larger specimens developed in the previous section to the substorm electron environment. The primary feature of this irradiation facility mounted in a 1.3 m diameter by 2.1 m long vacuum chamber is its dual beam electron flood gun capability. Each gun is capable of simultaneous irradiation of test specimens mounted at the opposite end of the chamber with electron energies from 0.5 keV up to 40 keV and at current densities in excess of 10 nA/cm<sup>2</sup> or as low as desired. Figure 27 shows a functional diagram of the system.

The 1.3 meter diameter by 2.1 meter long vacuum facility uses a combination of cryogenics and turbomolecular pumping to achieve a nominal operating vacuum in the  $1.3 \times 10^{-4}$  N/m<sup>2</sup> range. The interior of the system is shrouded with a high permeability foil for reduced

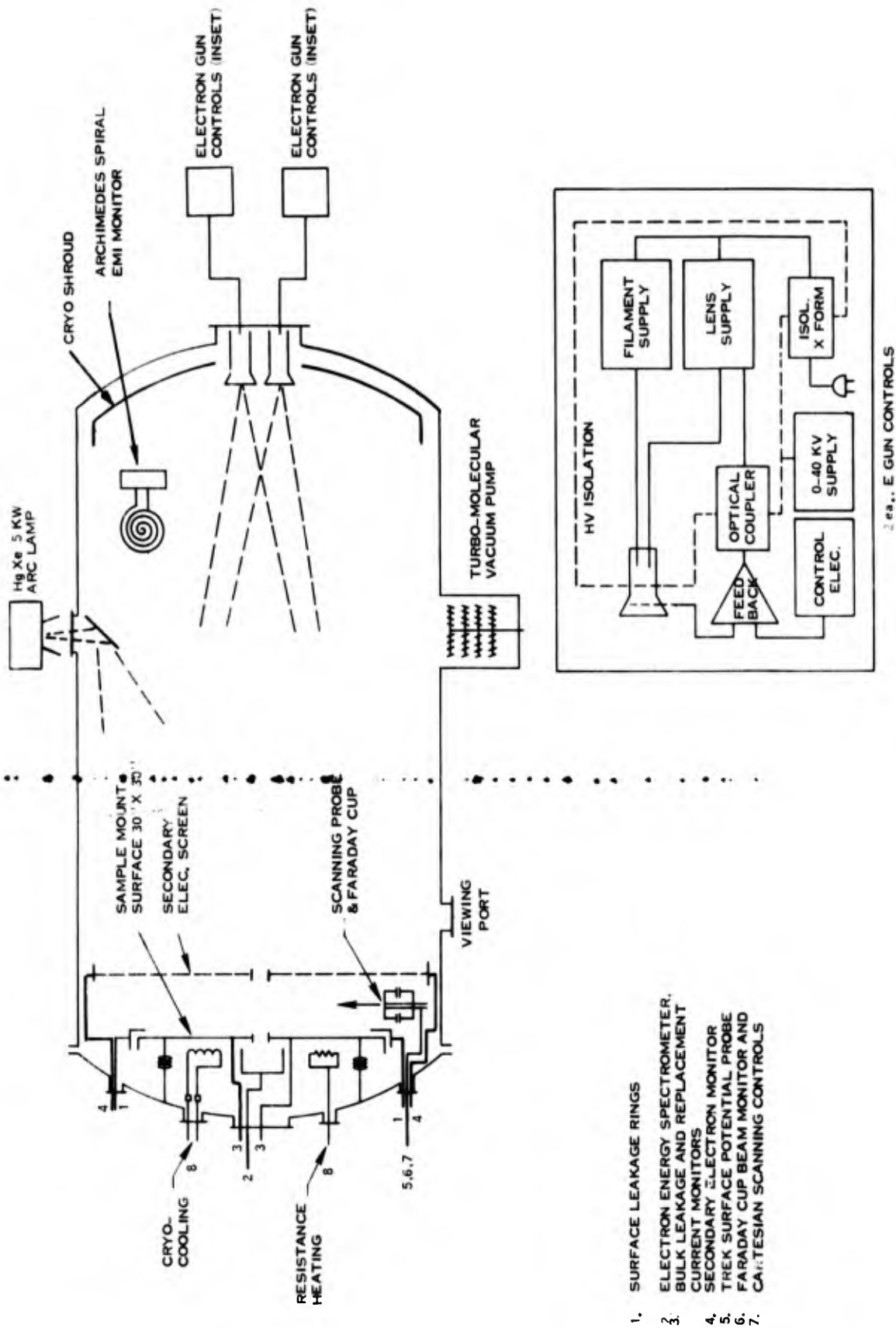


Figure 27. Functional Diagram of Multi Beam Facility

interference from external magnetic fields. The vacuum is monitored with an ion guage which is turned off during measurements to prevent photo emission effects from the gauge filament. A viewing port on the side of chamber which is normally covered is used for sample viewing and photographic recording of any ESD phenomenon.

All test samples and diagnostics are mounted on the "swing away" door of the vacuum chamber. The platform for the samples and all diagnostics is a 91 cm by 91 cm stainless steel reference ground panel mounted on the inside of the chamber door. This allows for easy access to samples requiring complicated handling techniques. The 91 cm square platform allows for simultaneous measurement of the performance of up to four 30 cm square samples.

The diagnostics system was assembled to measure the charge control characteristics of flat 30 cm square samples of conductively coated polymer films. The 30 cm (1 foot) square samples were mounted to aluminum plates which were electrically isolated from the stainless steel table with Teflon spacers. An aluminum electrode was placed around the perimeter of the sample to hold the sample in place and measure any surface currents. A schematic of the sample configuration is shown in Figure 28. Keithley 410 picoammeters are connected between the back plate and retaining ring and ground to measure surface and bulk or displacement currents. A wire mesh with a 90% transmission factor was suspended in front of the sample and grounded through another Keithley 410 picoammeter. The currents measured on this screen is a sum of 10% of the incident beam and the secondary emission of the sample. The screen may be floated above ground with batteries to increase the secondary emission pickup from the samples. The holding fixture supporting the wire mesh is positioned so as to mask the surface current electrode and expose a 29 cm square area to the electron beam. The schematic also shows the rotary arm whose axis is approximately at the center of 91 cm table. A Faraday mounted to the arm on a carriage which allows for its motion radially along the arm is used for measuring the current density across the sample. A Trek electrostatic surface voltmeter probe is also mounted on the rotary arm carriage for measuring surface potentials up to 20 kV anywhere on the surface. Figure 29 shows the actual sample configuration with the rotary arm. The Trek probe is not connected to the arm in this figure.

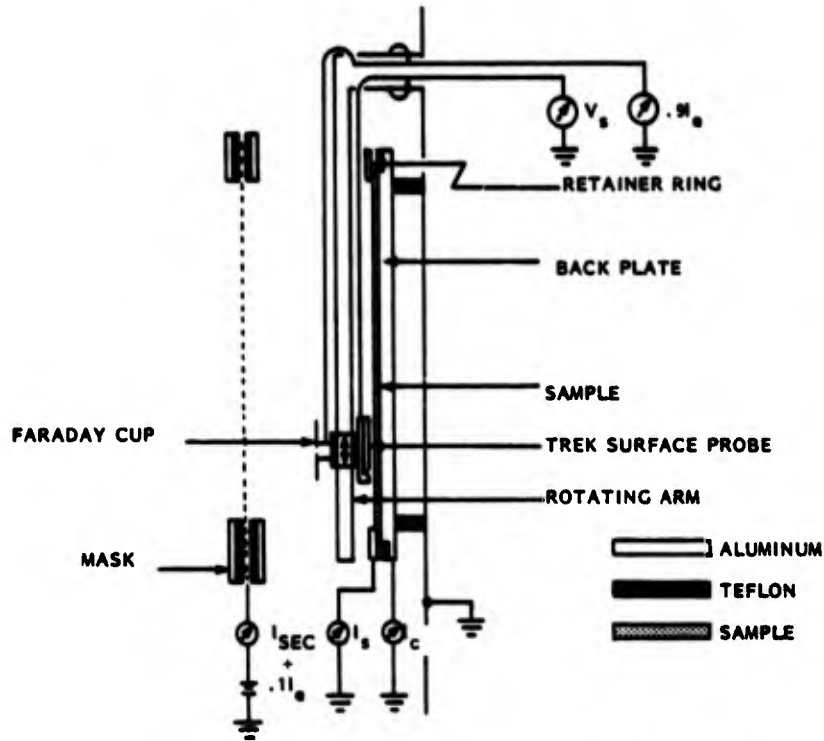


Figure 28. Schematic of Sample Configuration

## 2. VACUUM STABILITY

The stability of the indium-tin oxide coating on FEP Teflon was tested by placing sample no. 9 from Table 8 into the small ESD facility and monitoring its surface resistance under vacuum. The ESD facility was modified slightly in order to monitor the surface resistance of the ITO coating while it was under vacuum and also to measure the bulk, surface and secondary emission currents while the sample was irradiated. The 11.5 cm (4.5 inch) diameter sample was cut from sample no. 9 which had an average surface resistance of 70 Megohm. The surface resistance of the conductive coating was measured by placing a circular piece of conductive copper tape, 3M type X1181, in the center of the sample and soldering a 50  $\mu\text{m}$  wire to the copper tape as shown in Figures 30a and 30b. The metal ring which was placed around the perimeter of the sample normally for measuring the surface currents during the electron irradiation was used as the second electrode for measuring the surface resistance. The facility was modified for both resistance and irradiation measurements by using the ground bond in the center of the sample for measuring both surface resistance and surface currents during irradiation. A lead attached to surface ring was

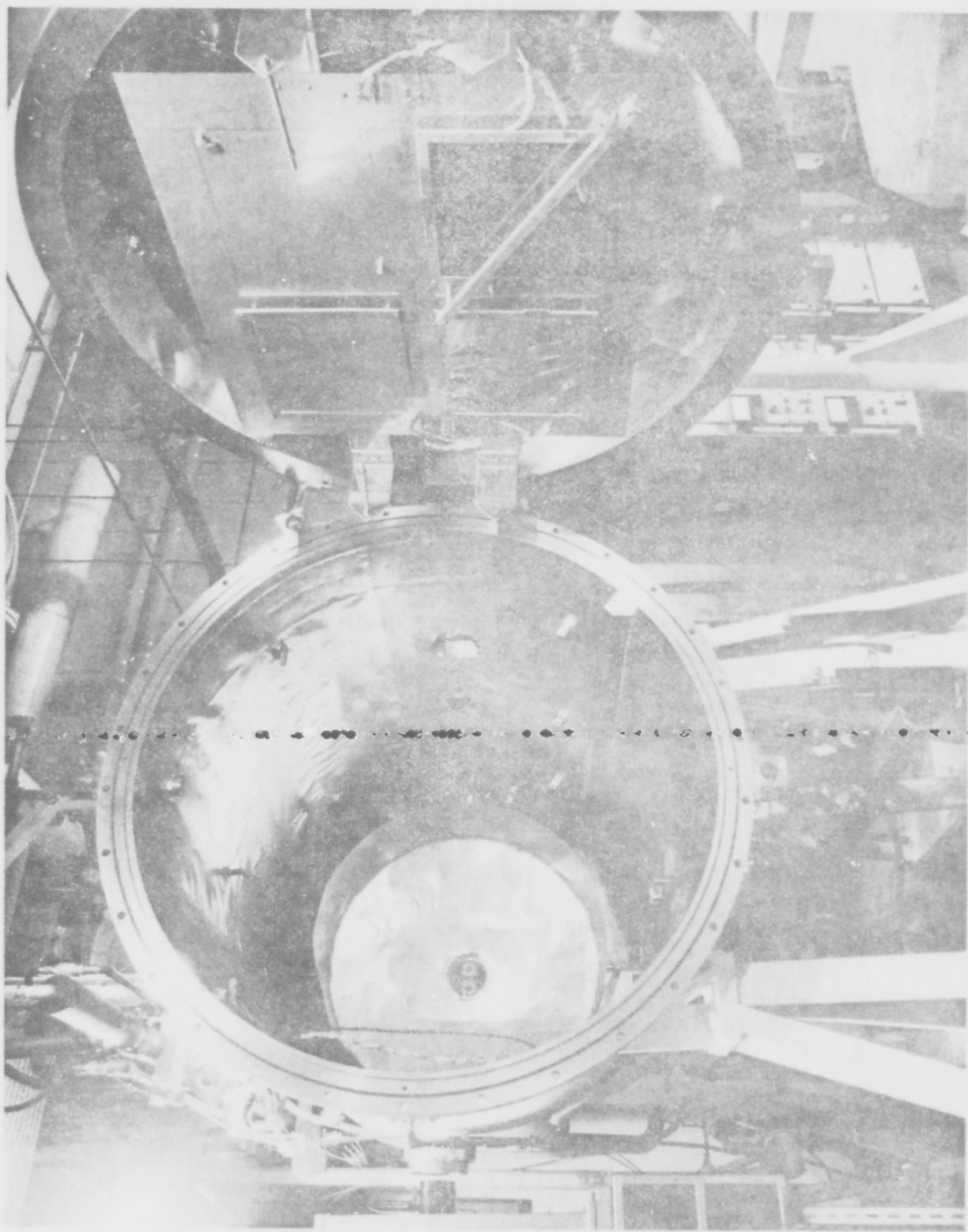


Figure 29. Actual Sample Configuration with Rotary Arm

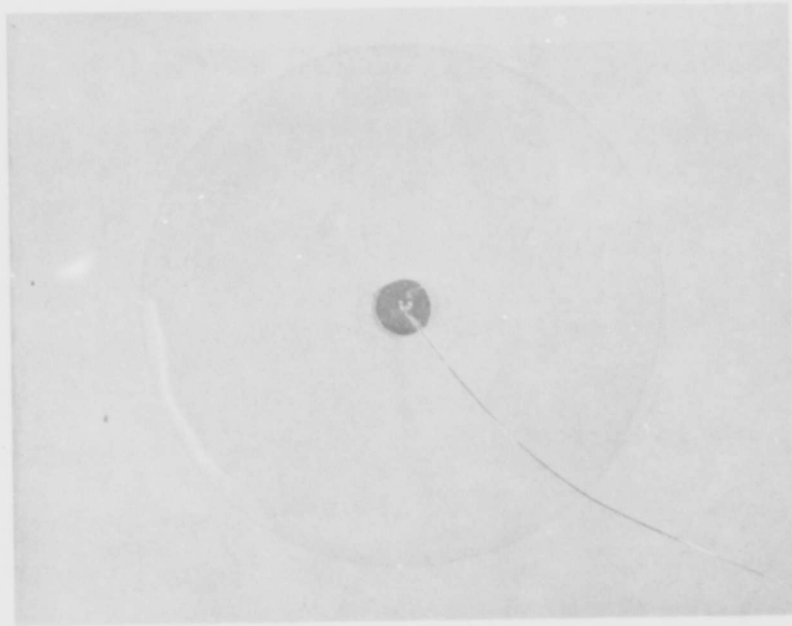


Figure 30a. ITO Coated FEP Teflon with Conductive Tape Ground Bond

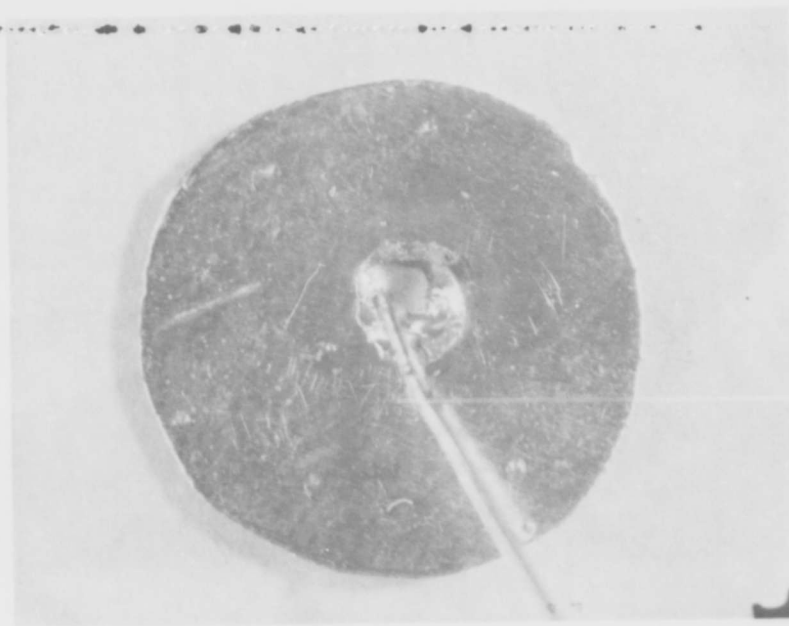


Figure 30b. Closeup of Conductive Tape Ground Bond on ITO Coated FEP Teflon

connected to a metal plug which was attached to but electrically isolated from the side wall of the chamber. The plug was located in such a position so that while the sample was not being irradiated the secondary electron collector cylinder could be swung to the side of the chamber and make contact with the plug. In this position the surface resistance of the ITO coating could be measured across the surface-current and secondary-electron-current feed-throughs of the ESD chamber. A Hewlett Packard high resistance meter model 4329A was used to measure the surface resistance of the sample in this configuration. After mounting the sample in the chamber, the surface resistance between the ground bond and perimeter of the sample was still about 70 megohms while at atmosphere pressure. After about six hours of pumping with the chamber in a low  $10^{-4}$  N/m<sup>2</sup> ( $10^{-6}$  Torr) range the surface resistance had decreased to about 1 megohm. After an additional eighteen hours, the vacuum was at  $1.2 \times 10^{-4}$  N/m<sup>2</sup> ( $9 \times 10^{-7}$  Torr) and the resistance had decreased to below 600 kilohms. Following these resistance measurements the sample was irradiated with electrons between 2 keV and 20 keV in energy. Table 15 summarizes the bulk, surface and secondary electron currents which were measured during the irradiation. Each irradiation was maintained for several minutes allowing the sample currents to stabilize. Following the irradiation, the surface resistance of the ITO coating was remeasured. With the exception of the measurement following irradiation by the 5 KeV electrons, the surface resistance remained approximately the same. The surface potentials were measured with the noncontacting Monroe electrostatic voltmeter probe which was swept across the surface of the sample following each irradiation. The maximum values were isolated to the area immediately above the solder connection of the ground wire to the copper tape shown in Figure 30b. Otherwise, the surface potential of the surface was negligible.

The stability of the  $100\text{\AA}$  indium tin oxide coatings on Kapton was also tested by placing a 11.5 cm (4.5 inches) diameter sample from deposition run no. 5 reported in Table 8 into the small electron irradiation facility and monitoring its surface resistance under vacuum. The ESD chamber had been modified as described above in order to measure both the surface resistance of the ITO coating before irradiation and surface and secondary emission currents during irradiation. The  $100\text{\AA}$  ITO coating had a surface resistance in the range of  $60\text{K } \Omega$  to  $80\text{K } \Omega$  at atmospheric pressure. The surface resistance dropped very quickly to about  $40\text{K } \Omega$  at a pressure of about  $10^{-1}$  Torr and remained relatively stable for the next six hours under nominal  $6 \times 10^{-6}$  Torr vacuum.

Table 15. Summary of Current Resistance Measurements on 11.5 cm Diameter ITO Coated FEP Teflon with Conductive Tape Ground Bond

Accelerating Voltage (kV)	$I_D^*$ (nA)	$I_R$ (nA)	$I_S$ (nA)	Max. Surface Potential (V)	Surface Resistance After Irrad. (K $\Omega$ )
-	-	-	-	-	600
2	<1	90	130	22	310
5	<1	190	80	38	1600
10	<1	240	65	41	290
15	<1	240	40	36**	400**
20	<1	260	60	38	550

\*\*After 30 minutes of continuous irradiation

\* $I_D$  = Displacement current in nA

$I_R$  = Surface current in nA

$I_S$  = Secondary electrons current in nA

### 3. LARGE AREA TESTING OF ITO

Twelve inch square sheets of indium-tin oxide coated 5 mil FEP Teflon and 3 mil Kapton were tested under electron irradiation in the 1.3 m by 2.1 m vacuum facility for spacecraft charging and radiation environments shown in Figure 31. The nominal operating pressure of the facility during the irradiation was  $1 \times 10^{-4}$  N/m<sup>2</sup> (0.8  $\mu$  Torr) which was achieved about 5 hours after closing the chamber.

Two 30 cm (1') square thin film samples with 200<sup>o</sup>Å of ITO on them were mounted as described in the first section. The sample configuration is shown in Figure 32 with the conductively coated FEP Teflon and Kapton samples mounted on the bottom fixtures. Also shown in

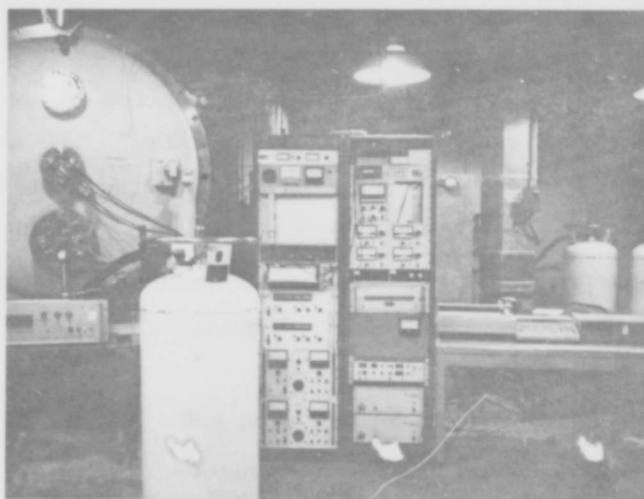


Figure 31. 1.3 Meter by 2.1 Meter Spacecraft  
Charging and Radiation Facility

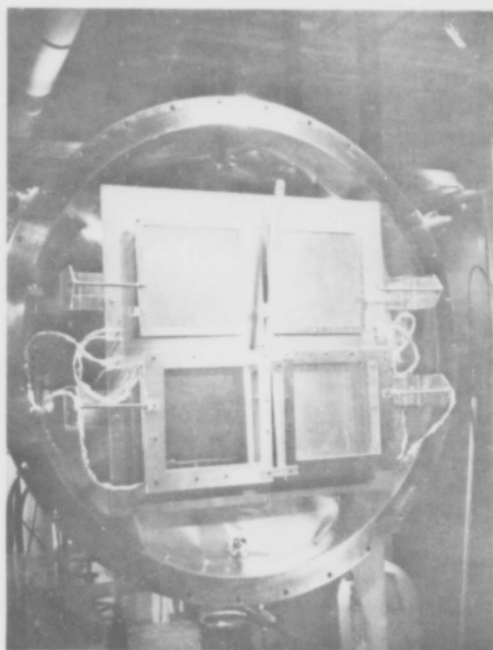


Figure 32. View of 12 Inch Square  
Sample Diagnostics Fixture

Figure 31 is a Faraday cup mounted to a rotary arm which was used for measuring the current density and mapping the electron flux distribution.

The 200 $\text{\AA}$  ITO coated polymer samples are reported in Table 5. The surface resistance of both samples were measured before mounting in the chamber and found to be in good agreement with those values reported in Table 5 which had been measured about 4 weeks earlier. The conductively coated samples were irradiated in monoenergetic electron beams between 5 keV and 40 keV at an average current density of about  $0.2 \text{ nA/cm}^2$ .

The displacement and surface currents for the two samples were measured and recorded simultaneously for the first several minutes of irradiation. The secondary emission current and surface potentials were not measured during these initial measurements of the large area samples. Table 16 summarizes the displacement current and surface currents measured on the two samples. The displacement and surface currents were not measured on the Kapton sample at the 30 keV and 40 keV accelerating voltages because of intermittent noise problems which arose after the first set of measurements. No discharges were observed on either of the measured currents for both the ITO coated FEP Teflon and Kapton samples. The shape of the displacement currents initially were similar to those observed in the smaller samples. That is, a small initial subsurface charging pulse was observed for most of the voltages tested along with a corresponding but slightly smaller negative pulse occurring when the accelerating beam was turned off.

The 200 $\text{\AA}$  ITO coating on the 30 cm (12 inches) squares of  $75 \mu\text{m}$  Kapton and  $12.5 \mu\text{m}$  FEP Teflon was retested after the noise problems, which were encountered in the initial measurements, were resolved by locating several ground loop problems and adding shielding to several exposed dielectric covered wires. Table 17 summarizes the surface and conduction currents through the ITO coated  $12.5 \mu\text{m}$  FEP Teflon and  $75 \mu\text{m}$  Kapton.

The average current density for these measurements was increased to about  $2 \text{ nA/cm}^2$ , about 10 times greater than the values used for the previous experiment. A change of direction in the electron current was observed in the  $75 \mu\text{m}$  Kapton between 1 and 2 kV. This behavior is

Table 16. Summary of Current Measurements on One Foot Square Samples of ITO Coated FEP Teflon and Kapton

Accelerating Potential (kV)	ITO/Kapton		ITO/FEP Teflon	
	I <sub>D</sub> *	I <sub>R</sub> *	I <sub>D</sub>	I <sub>R</sub>
5	8	43	2	80
10	4	70	.6	90
15	8	80	.3	90
20	8	100	.3	95
30	-		.6	90
40	-		.6	110

\*I<sub>D</sub> = Displacement Current in nanoamperes

I<sub>R</sub> = Surface Current in nanoamperes

Table 17. Summary of Current Measurements on ITO Coated Kapton and FEP Teflon Films

Beam Voltage (kV)	ITO/Kapton (75 μm)		ITO/FEP Teflon (12.5 μm)	
	Surface Current (nA)	Bulk Current (nA)	Surface Current (nA)	Bulk Current (nA)
1	720	-75	28	32
2	230	52	36	25
3	270	48	40	18
4	800	37	55	13.5
5	1200	29	84	10
7.5	1500	26	110	7.6
10	1600	25	125	7.3
15	1650	24	150	7.8
20	1700	24.5	170	8.8
30	1800	26	210	10.5

due to the variation in secondary emission of the Kapton as a function of incident electron energies.

A second set of measurements were made on  $100\text{\AA}$  ITO coatings on one foot square samples of FEP Teflon and Kapton. The samples were taken from the same set of samples as the above materials. These samples were chosen because their coatings had higher surface resistances than the  $200\text{\AA}$  coatings. Surface resistance measurements of the ITO coated Kapton had a resistance from center to edge in the range of 19 to 25K  $\Omega$  while the ITO coating on the sheet of Teflon had a resistance from center to edge of the order of  $4 \times 10^9$  ohms.

The conductively coated samples were irradiated in a monoenergetic beam between 1 keV and 30 keV at an average current density of about  $1 \text{ nA/cm}^2$ . The displacement on bulk and surface currents for the two samples were measured and recorded simultaneously for the first several minutes of irradiation. The current through the secondary electron collector screens were also recorded for these measurements. Table 18 summarizes the current measurements from the two samples. The currents from the samples were monitored for several minutes during the irradiation and no discharges were observed on any of the currents from either the coated FEP Teflon or Kapton samples. A small initial spike in the displacement current was observed for accelerating voltages above 5 kV when the electron gun was turned on indicating small subsurface charging but no discharges were observed.

#### 4. MULTIPLE ENERGY EXPOSURE

Two  $100\text{\AA}$  thick indium oxide coated 30 cm (12 inches) square samples, one silvered FEP Teflon and one aluminized Kapton, were tested in the 1.3 m by 2.1 m static charging and radiation facility. The samples had a fairly uniform distribution of surface resistances over the entire 30 cm (1') square. The surface resistance on the  $75 \mu\text{m}$  Kapton substrate was between 5 and 8 k  $\Omega/\square$  and between 14 and 50 k  $\Omega/\square$  on the  $125 \mu\text{m}$  FEP Teflon.

Table 18. Summary of Current Measurements on One Foot Square Samples of 100Å ITO Coated FEP Teflon and Kapton

Accelerating Potential (kV)	ITO/Kapton			ITO/Teflon		
	$I_D^*$ (nA)	$I_S$ (nA)	$I_{SEC}$ (nA)	$I_D^*$ (nA)	$I_S$ (nA)	$I_{SEC}$ (nA)
1	17	335	.54	7.9	4.5	0.26
2	14.7	183	.28	8.0	11.8	0.4
5	11	370	2.1	9.4	26.0	1.45
10	2.75	335	21	5.1	22.0	2.4
20	2.3	335	28.5	4.0	28.5	3.3
30	2.3	345	30	7.4	30.5	4.0

$I_D$  = Displacement and bulk current  
 $I_S$  = Surface current  
 $I_{SEC}$  = Screen current

The conductively coated samples were irradiated in a monoenergetic beam between 2 keV and 30 keV at an average current density of about  $1.5 \text{ nA/cm}^2$ . The bulk displacement and surface currents for the two samples were irradiated for several minutes and the currents recorded. Table 19 summarizes the measured currents from the two samples. No electrostatic discharges were observed by visual inspection of the sample during irradiation or detected in the recorded currents.

Following irradiation of 30 keV, the samples were irradiated by 2 keV electrons from the same electron gun to determine the reproducibility of the data at previously measured electron energies.

The other electron gun was then used to irradiate the samples at 20 keV to measure its performance in a monoenergetic environment prior to irradiation in a dual energy environment. Table 19 also includes the measured currents from irradiation by the second electron gun. In both cases, the bulk currents remained in the 2 to 6 nA range for the entire sample for either material with the surface coating accounting for most of the remaining electron flux.

Table 19. Summary of Current Measurements on 100<sup>0</sup>Å Indium Oxide Coated Kapton and Teflon Films

Beam Voltage (kV)	IO/KAPTON/Al (75 μm)		IO/FEP Teflon/Ag (12.5 μm)	
	Surface Current (nA)	Bulk Current (nA)	Surface Current (nA)	Bulk Current (nA)
(gun #1) 2	14.2	11.6	13.4	8.7
5	112.0	6.1	56.0	5.2
10	130.0	3.8	56.5	2.7
15	167.0	4.5	80.0	3.0
20	127.0	3.6	86.0	2.9
30	125.0	4.7	96.5	2.9
2	12.5	9.7	8.6	7.8
(gun #2) 20	320.0	5.9	39.0	2.5
(gun #1) + (gun #2) 2                      20	175	9.6	27.5	6.8

Both electron guns were then used to irradiate the indium oxide coated samples, one at 2 keV and the other at 20 keV. The currents are summarized in Table 19. Both electron guns were set to electron flux levels used in the previously recorded measurements.

Since this initial set of tests on the 100<sup>0</sup>Å IO coatings were made without the secondary electron collector or electrostatic voltmeter in the system, the measurements were then repeated with these in place. The secondary electron collector was constructed of a 90% transmission wire mesh suspended about four inches in front of the test specimen. It was held in place by and isolated from a grounded plate which formed a mask in front of the sample restricting the incident electrons to the area of the sample and shielding the surface current electrode around the perimeter of the sample. The effective irradiated area of the test specimens was about 840 cm<sup>2</sup> (29 cm)<sup>2</sup>. A Faraday cup mounted to a rotary arm whose

axis was approximately in the center of the 36-inch square test fixture reference ground plane was used to measure the beam current density over the sample. A Trek capacitively-coupled electrostatic voltmeter probe was also mounted to the rotary arm across from the Faraday cup. The surface probe was positioned so as to sweep about 1 cm above the surface of the test specimen. The probe was calibrated at this distance against an insulated flat plate which was held at 1 kilovolt and was found to track the surface voltage within 2%.

The conductively coated samples were then irradiated in a monoenergetic electron beam between 0.5 and 35 keV. The samples were irradiated for several minutes until the bulk, surface and secondary screen currents stabilized and were then recorded. Table 20 summarizes the measured currents from the two samples.

Table 20. Summary of Currents from  $100\text{\AA}$  IO Coated Kapton and Teflon Films

Accelerating Voltage (kV)	IO/Kapton/Al (75 $\mu$ m)			IO/FEP Teflon/Ag (125 $\mu$ m)		
	Surface Current (nA)	Bulk Current (nA)	Screen Current (nA)	Surface Current (nA)	Bulk Current (nA)	Screen Current (nA)
(Gun #1)						
0.5	-193	50	0.06	16	20	0.5
1	- 87	33	0.05	17	21	0.5
2	0.4	22	0.2	17	18	0.6
3	60	24	7	25	16	1.2
4	93	24	1.5	53	13	2.0
5	112	20	2.6	79	11	2.9
7	125	12	5	104	9	4.3
10	136	8	10	114	6.5	7
15	140	10	13	120	6.5	10
20	128	10	13	127	6.4	11
25	158	12	16	130	6.5	14
30	166	10	16	148	6	14
35	182	9	18	153	5.5	15
(Gun #2)						
10	176	26	11	30	1.8	2.2
20	172	1.8	13	43	1.3	3.5
(Gun #1)+(Gun #2)						
1 10	74	39	0.3	24	24	0.8
2 20	196	36	1.2	46	21	1.3

High negative values were observed at low accelerating potentials in the surface currents on the IO coated Kapton sample. This is similar to what has been previously observed in ITO coated Kapton films reported earlier at the higher current densities. Figure 33 shows a plot of the normalized currents from the two samples. The negative total current at the low incident electron energies of 0.5 and 1.0 keV implies that all of the electrons incident on the sample are not being measured. A much higher secondary electron current should be observed than was actually measured indicating that all the secondaries are not being collected by the screen.

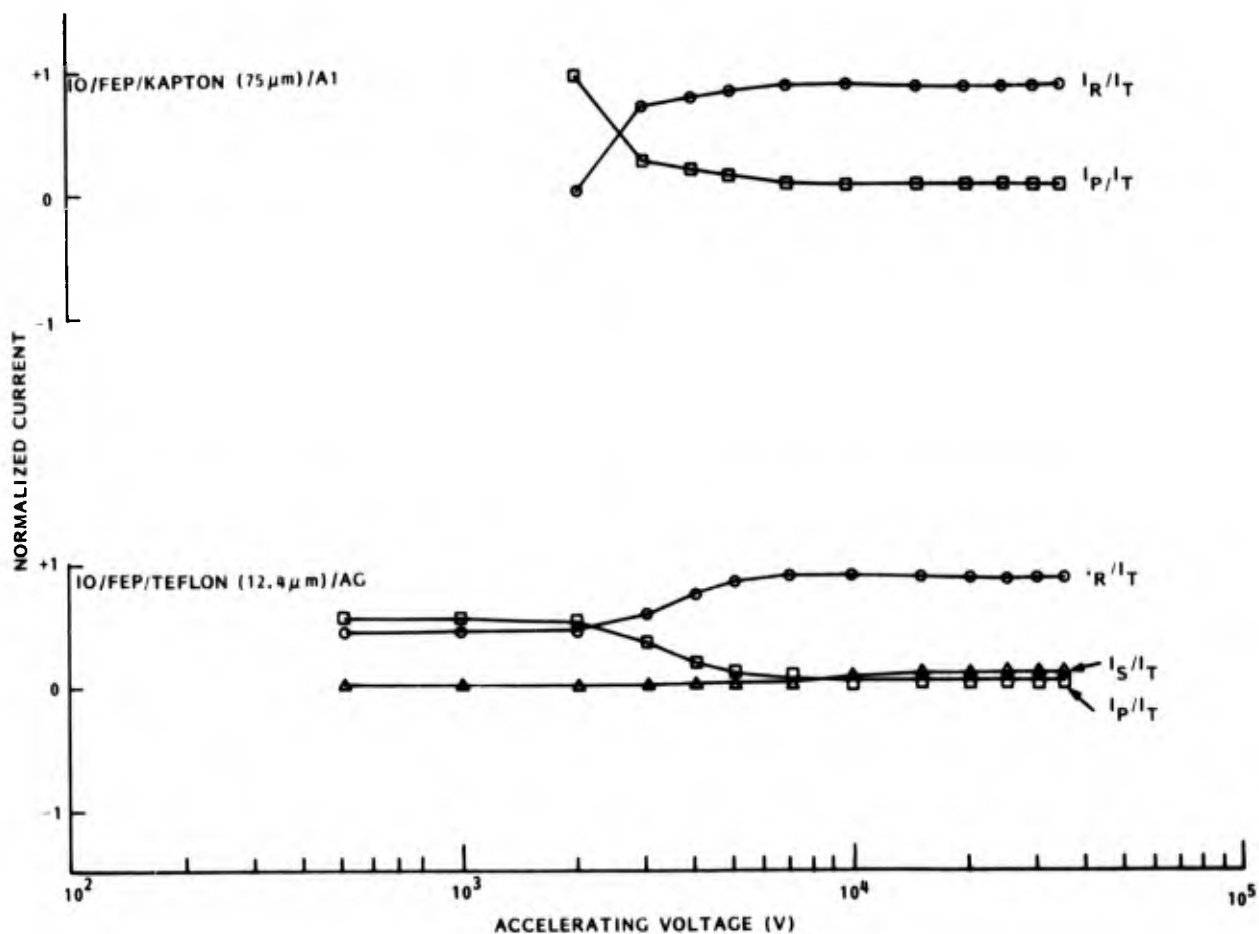


Figure 33. Normalized Charging Characteristics of IO Coated FEP Teflon and Kapton

Following stabilization of the currents being measured, the Trek probe was swept across the sample. The sweep was made while the electron beam was on. Before and after each sweep, the probe reading was checked by positioning it over a grounded plate. The probe was swept

in a single arc across the approximate center of the 30 cm square samples. No significant surface potentials were measured on either of the IO-coated samples. Surface voltages up to about +30 volts were recorded on the IO coatings on both the Kapton and FEP Teflon while being irradiated by electrons above 20 keV. However, voltages returned to near zero after the beam was turned off.

A third set of measurements were made with a +90V bias on the secondary screen in order to account for the apparent electron imbalance. The secondary screen current increased significantly but not sufficiently to account for the high negative current through the aluminum ring around the surface perimeter. Additional analysis of the system and measurements are required to account for the apparent imbalance in the distribution of currents.

#### 5. LOW TEMPERATURE STABILITY

The 100Å indium oxide coated aluminized Kapton sample tested in the previous section was retested at low temperatures to determine the stability of the coating at reduced temperatures expected for typical thermal control materials. The sample was mounted on the same aluminum plate as used before. However the 91 cm square stainless steel table was replaced by a 76 cm by 100 cm cryopanel as shown in Figure 34. For measuring the surface resistance of the sample the surface electrode around the entire perimeter of the sample was replaced by two sections of the ring which were formed by cutting out two opposite sides. This left two strips of the ring on either side of the sample which were about 30 cm wide and about 29 cm apart. The surface resistance was then the resistance between these two electrodes directly in ohms per square. The sample was then mounted to the cryopanel and the surface resistance was measured between 60 and 120 k $\Omega$ . No significant change was observed in surface resistance of the sample as the pressure was lowered to the mid  $10^{-4}$  N/m<sup>2</sup> (1  $\mu$  Torr) range.

The temperature of the IO coated Kapton sheet was lowered by putting LN<sub>2</sub> into the cryopanel and radiative cooling the sample holder. The surface resistance of the sample was monitored occasionally as the sample temperature was lowered to -78°C (-172°F) at which it stabilized between 9 and 36 k $\Omega$ . The value of the surface resistance seemed to become more stable at the lower temperatures. The IO coated thin film was then irradiated with electrons between 1 and 24 keV at an average current density of 1nA/cm<sup>2</sup>. The two surface electrodes were tied

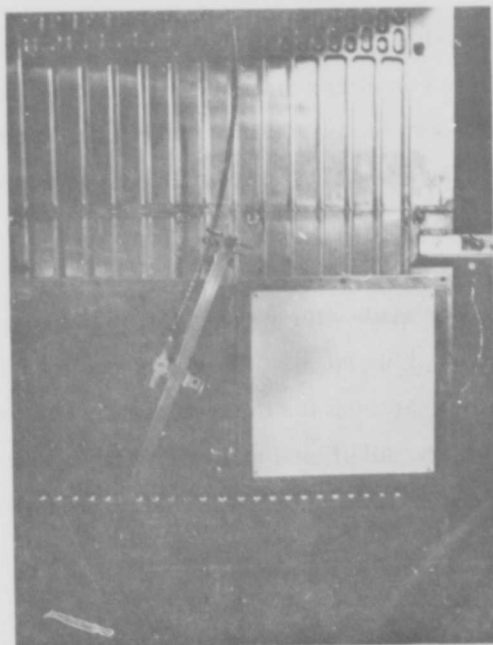


Figure 34. 76 cm by 100 cm Cryopanel

together for monitoring surface currents but were not recorded. Following stabilization of the bulk and surface currents the Trek surface potential probe was sweep across the sample. The surface voltages were consistently below -5 to -10 volts. Following the irradiation at 6 keV, 12 keV and 20 keV the surface resistance of the conductive coating was measured. No significant difference was measured from the initial  $9\text{ k}\Omega$  value.

## SECTION IV CONCLUSION

Highly stable, low resistance, low absorptance thin coating of indium-tin oxide and indium oxide have been successfully and repeatedly deposited on thermal control substrate materials typically used on external spacecraft surfaces. The development and evaluation of thin indium oxide and indium-tin oxide coatings on aluminized Kapton, silvered FEP Teflon, OSR and solar cell coverglasses have established a high degree of confidence about their characteristics, use and the dependence on the processing parameters required to achieve a conductive and high transmittance coating.

Magnetron sputtering from the indium and indium tin targets in an oxygen atmosphere was chosen early in the program as the prime deposition technique because of its advantages over other techniques. The works reported here has verified some of these characteristics which include:

- low substrate heating
- large deposition area
- better coating adhesion
- more easily controlled deposition rate
- greater uniformity

These characteristics and others have also been identified by others.<sup>8</sup> Furthermore, reactive sputtering from metal alloy target has been shown to provide repeatable depositions from sources which are less expensive to fabricate and operate than from oxide targets.<sup>9</sup>

---

<sup>8</sup> Recent Developments in Sputtering - Magnetron Sputtering, John A. Thornton, Metal Finishing 77(4), 1979, pg 45-49.

<sup>9</sup> The Sputtered Indium Tin Oxide Film, Vance Hoffman, Optical Spectra, pg 60-62, November 1978.

Results show that optimum transmission and solar reflectance and performance in a radiation environment can be obtained only by minimizing the thickness of the applied coating. The optimal thicknesses must be determined by balancing the deposition capability and handling characteristics with a resistivity and solar absorptivity stability sufficient to achieve charge control.

Conductive transparent coatings of IO and ITO have been reproducibly deposited in thickness between  $100\text{\AA}$  and  $1000\text{\AA}$ . Storage, handling and environmental testing indicate that  $200\text{\AA}$  coatings can be reproducibly deposited and provide highly stable semi-conducting properties with solar absorptances of one or two percent. The coatings applied to glass, FEP Teflon and Kapton substrates have consistently been in the low  $\text{k}\Omega/\text{square}$  range.

The effect of oxygen partial pressures, deposition rate and insitu biasing of the planetary on the coatings performance have been investigated. Because of the nature of the sputtering process, particularly for nondedicated systems, exact values of the process variables cannot be specified. However, the general dependence between process variables and coating performance have been established so that the chamber conditioning period required to obtain consistent coatings is minimized.

Indium tin oxide and indium oxides have been evaluated together under combined environments. Results indicate the indium tin oxide coatings have slightly better optical properties than the indium oxide coating of the same thickness but are not as stable.

Surface resistances of both coatings have been shown to be very stable with reasonable humidity and temperature control. Typical changes of the order of one magnitude have been observed but absolute values have always been several orders of magnitude in resistance lower than that required for successful charge control. Similar changes have been observed in the coating resistance while under vacuum and radiation environments.

All radiation measurements of the coatings under simulated substorm condition have exhibited the characteristics of stable charge control. Measurement of surface potentials during and after irradiation by electrons up to 30 keV in energy show an effective grounded surface with no evidence of charge buildup or discharging. Synergisms in the current distribution between surface, bulk and secondary emission appear in data recorded using multiple low electron irradiation but charge control properties are maintained without any degradation to the surface potential.

THIS REPORT HAS BEEN DELIMITED  
AND CLEARED FOR PUBLIC RELEASE  
UNDER DOD DIRECTIVE 5200.20 AND  
NO RESTRICTIONS ARE IMPOSED UPON  
ITS USE AND DISCLOSURE.

DISTRIBUTION STATEMENT A

APPROVED FOR PUBLIC RELEASE,  
DISTRIBUTION UNLIMITED.

---